THE UNIVERSITY OF MANITOBA

A SIMPLIFIED METHOD OF MODELLING COMPLEX POWER SYSTEMS

by

GERALD J. RHEAULT

A THESIS

SUBMITTED TO THE FACULTY OF GRADUATE STUDIES

IN PARTIAL FULFILMENT OF THE REQUIREMENTS FOR THE DEGREE

OF MASTER OF SCIENCE

ELECTRICAL ENGINEERING

WINNIPEG, MANITOBA

October 1973

ABSTRACT

This investigation concerns a novel analog computer power system model, which incorporates the power angle sine curve representing power flow along a transmission line as a function of the voltage phase angle difference of the line. Once built, this non linear approximate representation is tested in a power and frequency control loop by applying step voltage disturbances and recording the behavior. The behavior is compared with that of a digital computer simulation of the same system subjected to the same disturbances.

ACKNOWLEDGEMENT

The author wishes to acknowledge his indebtedness to Professor G. W. Swift for his never failing guidance and assistance and to Professor M. Z. Tarnawecky for his interest and encouragement. Thanks also to Mr. C. J. Goodwin for agreeing to review this manuscript. Thanks are also due to Mrs. Donna Pittet for an expertly typed manuscript.

The financial assistance of the National Research Council and Manitoba Hydro is also gratefully acknowledged.

TO MY MOTHER

WITH DEEP GRATITUDE AND AFFECTION

TABLE OF CONTENTS

		Page
ABSTRACT		ii
ACKNOWLEDGEMENT		iii
DEDICATION		iv
LIST OF TABLES		vii
LIST OF ILLUSTRATIONS		viii
LIST OF SYMBOLS		x
CHAPTER		
I	INTRODUCTION	1
II	THEORY OF SINE CURVE POWER/ANGLE REPRESENTATION	4
	2.1 The Power Flow Equation	4
	2.2 Power Relation for a Synchronous Machine	5
	2.3 Effect of Line Resistance on Power Flow Equation	8
III	THEORY AND DESIGN OF SINE CURVE NON-LINEAR ELEMENT	15
	3.1 Theory of Sine Curve Nonlinear Element	15
	3.2 Design of Sine Curve Nonlinearity	23
	3.3 Building of Diode Function Generator	25
IV	SYSTEM MODELS	35
	4.1 Modelling of the Fundamental Two-Bus System	35
	4.2 Addition of Turbine and Governor Dynamics to Fundamental Two Bus System	40
	4.3 The Two-Area System	43
V	PRESENTATION AND COMPARISON OF RESULTS	51
	5.1 Description of Techniques used in Running Tests	51
	5.2 Results from the Fundamental Two Bus System	51
	5.3 Results for Fundamental Two Bus System With Governor and Turbine Included	55
	5.4 Results of a Two-Area Simulation	61
VI	CONCLUSION	69

Page

APPENDIX

A DERIVATION OF POWER LOSS TERM 74

B LEAST-SQUARED ERROR ANALYSIS PROGRAM 76

C CSMP PROGRAM FOR SWING EQUATION MODEL 77

D CSMP PROGRAM FOR TURBINE AND GOVERNOR INCLUDED MODEL 78

E CSMP PROGRAM FOR TWO-AREA MODEL 79

BIBLIOGRAPHY 71

LIST OF TABLES

		Page
TABLE I -	Configurations Tested to Determine Design Parameters	26
TABLE II -	List of Step Voltage Stability Limits for Fundamental Two Bus Model	54
TABLE III -	List of Step Voltage Stability Limits for Turbine and Governor Model	60
TABLE IV -	List of Step Voltage Stability Limits for Two-Area Model	62

LIST OF DIAGRAMS

Figure		Page
1-1	Block Diagram of a System Study Method	3
2-1	Comparison of Steady State and Transient Generator Power	7
2-2	Single Line Diagram	8
2-3	Simplified Single Line Diagram	8
2-4	Comparison of Lossy and Lossless Case	12
3-1	Use of Straight Line Approximations	16
3-2	Sine Wave with Straight Line Segments	17
3-3	Simplified Functional Diagram of DFG	17
3-4	Input Output Relationship of the Circuit of Figure 3-6B	20
3-5	Demonstrates the Generation of an Arbitrary Slope by the Circuit of Figure 3-6C	20
3-6	Different Types of Diode Function Generators	21
3-7	Circuits used for Visual Representation	27
3-8	Ideal Line Segments	28
3-9	Diagram Showing Connections to be Made on the Analog Computer	30
3-10	Diode Function Generator Circuit Schematic	31-32
3-11	Output of DFG X-Y recording of DFG Output	34
4-1	System Block Model	38
4-2	Analog Model of a Two-Bus System	39
4-3	CSMP Model of a Two-Bus System	39
4-4	Model for Governor and Turbine	41
4-5	Combination of Governor and Turbine Transfer Function	42

Figure | Page

4-6 Complete Block Diagram of System with Turbine and Governor Model Included for the system.....44

4-7 TR-20 Analog Computer Diagram of Model with Turbine and Governor.....45

4-8 CSMP Diagram of Model with Turbine and Governor.....46

4-9 TR-20 Analog Model of Two-Area System.....49

5-1 P_e vs Time for Two-Bus Model.....52

5-2 δ vs Time for Two-Bus Model.....53

5-3 P_e vs Time for Governor and Turbine System Model.....57

5-4 δ vs Time for Governor and Turbine System Model.....58

5-5 Output Trace for Step Input Causing Instability.....59

5-6 P_e vs Time for Two-Area Model with Step Input at P_{m1}.....63

5-7 δ vs Time for Two-Area Model with Step Input at P_{m1}.....64

5-8 P_e vs Time for Two-Area Model with Step Input at P_{m2}.....65

5-9 δ vs Time for Two-Area Model with Step Input at P_{m2}.....66

LIST OF SYMBOLS

D	damping constant
D_1, D_2	damping constant for swing equation of areas A and B
E	internal EMF of the machine
H	inertia constant
I	internal current of the generator
I_q	quadrature axis current of the generator
I_d	direct axis current of the generator
K_g	governor gain term
K_t	turbine gain term
M	momentum constant for swing equation
M_1, M_2	momentum constants for swing equation of areas A and B
P_{ab}	power output at the sending end terminal from bus A to bus B
P_e	real power output from bus B to bus A
P_g, Q_g	the real and imaginary component of complex generator power
P_L	power loss along a transmission line due to resistance
P_m	mechanical power to the system
P_{m1}, P_{m2}	mechanical power to the system at area A and area B
Q_{ab}	reactive power output from bus A to bus B
Q_{ba}	reactive power output from bus B to bus A
S	Laplace transform variable
S_{ab}	complex power flow from bus A to bus B

S_g	complex power of a generator
T_g	governor time constant
T_t	turbine time constant
V	terminal voltage of generator
V_a, V_b	magnitude of sending end and receiving end voltages at buses A and B
X	reactance of line connecting the two terminals
X_d	direct axis reactance of generator
X_q	quadrature axis reactance of generator
δ	angular position
δ_{ab}	angular position of the voltage of bus A with respect to bus B
ϕ	phase angle between voltage and current of the machine
θ	power factor angle
ω	frequency of the system

CHAPTER I: INTRODUCTION

Power system modelling is a very important aspect of power system work. The planning engineer relies on system models of various kinds to help him determine system behavior and characteristics. He uses them to determine loading patterns on parts of the system, stability of the system under various loads and faults, and control studies on plants and individual generators. All of these models consist of mathematical equations that have been conceived to represent the behavior of the system. None of these models is exact in representing the system but the models are close enough to be quite useful for the purposes of the planning engineer.

These mathematical models consist of differential and partial differential equations, and methods of solving them either for exact or approximate solutions must be found. With the advent of digital computers, approximate techniques for solving the equations have been developed, using the high speed repetitive ability of the machines. Also, analog computers offer methods of providing solutions, but in most cases the size of the machine required to solve the equations associated with a fairly large system makes their use impractical. In a paper published by Sokolov, Gurevich and Khvoshchinskaya "A New Method of Studying Large Complex Power Systems on Analogue Computers" [16] they suggest analog methods of simulating different parts of the power system under study. This system model can be used to perform the different kinds of studies (i.e. load flow, stability, fault study) required.

In this same reference, the authors present the idea of using line segments connected to one another to produce the sine curve power flow equation nonlinearity. This is the same technique used in this thesis to represent the nonlinear behavior of power on the transmission system. A part of this project consisted of designing and building an accurate nonlinear function circuit which will hopefully be useful in future power system control studies. The first part of the thesis consists in justifying the presence of such a nonlinearity in the power frequency control loop. Once the function's validity has been proven the nonlinearity is designed and built. The third and final part of the exercise consists in using this nonlinear element in a power and frequency control model and comparing the resultant analog output with digital computer results of a simulation of the same model, but using an exact sine wave representation.

The future trend in power systems is to installing mini-computers in generating stations to perform all the control and protection functions in that plant. Minicomputers are computing machines which typically have fast processing rates, relatively short word lengths, versatile input-output structures and are used in dedicated real time types of applications. But before such a machine can be used for control purposes its effect on system operation must be studied.

A number of ways of determining this system behavior are available. They are, 1) connect the minicomputer to the real system and under various disturbance conditions determine the effect of the minicomputer controller

2) perform a digital simulation in which the complete system is modelled on a large digital computer and interfaced to the minicomputer and

3) use a hybrid approach where the system is modelled on an analog computer and this analog machine is interfaced by A/D and D/A conversion to the minicomputer.

The first of these methods is totally impractical because of the disruptive effects the tests would have on the operation of the system. The second test is feasible but the costs involved in modelling the whole system and the troubles of interfacing two digital computers make it less desirable than method three. Method three, on the other hand is faster and cheaper than the all-digital one. In this method, as illustrated in Fig. 1.1, an analog or hybrid computer is used to model the system, and to it is connected a minicomputer through A/D and D/A conversion equipment. The system model developed and tested in this thesis would be the analog portion of the system if it was attempted to have a minicomputer control the power flow and frequency of a generator or plant.

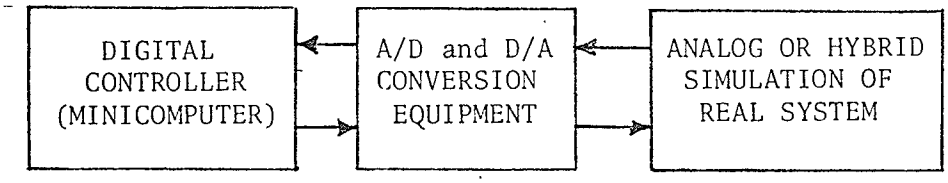

Fig. 1-1 Block Diagram of a System Study Method

CHAPTER II: THEORY OF SINE-CURVE POWER/ANGLE REPRESENTATION

2.1 The Power Flow Equation

For tie lines or other forms of transmission network in a power system, constraints as defined by transmission line parameters, provide an upper bound to the stable operation of the system. These constraints define the maximum power that can be transferred between two points of the system. For given sending end and receiving end terminal voltages, the power transfer through a tie of zero resistance is given by

$$P_{ab} = \frac{V_a V_b}{X} \sin \delta_{ab} \qquad (1)$$

where P_{ab} is the power output at the sending end terminal (equal to the power input at the receiving end terminal), V_a and V_b are the magnitudes of the sending end and receiving end voltages; X is the reactance of the line connecting the two terminals; and δ_{ab} is the difference in the phase angles of the two voltages. From Eqn 1 the power limit of the line is

$$P_m = \frac{V_a V_b}{X} \qquad (2)$$

This point occurs where the phase angle of the sending end voltage leads the phase angle at the receiving end by 90°.

As far as the transmission system between any two areas is concerned, Eqn 2 indicates that the power limit of the tie can be increased by

increasing the terminal voltages or by decreasing the line reactance (increasing the voltage level, adding a parallel circuit, changing from single to bundled conductor, etc.). Conversely any disturbance causing a reduction in voltage or an increase in the impedance between the terminals will result in a corresponding reduction in the amount of power that can be transferred between two areas.

2.2 Power Relation for a Synchronous Machine

The next question asked relates to the real and reactive power consumed or delivered by the synchronous machine. This formula is derived in reference 34 pages 96-99, to be the following

$$P_g = \frac{|V||E|}{X_d} \sin\delta + \frac{|V|^2}{2}\left(\frac{1}{X_q} - \frac{1}{X_d}\right) \sin 2\delta$$

where

P_g = steady state power out of the generator

V = terminal voltage of generator

E = internal EMF of the generator

X_d = direct axis reactance of the generator

X_q = quadrature axis reactance of the generator

δ = angular position of the generator rotor referenced to some fixed angle

This equation applies to the steady state operating condition of the generator whereas in this study an equation for the transient behavior is required.

Under transient conditions

$E \rightarrow E'$ and

$$X_d \rightarrow X'_d$$

where

E = pre-fault EMF of the generator

E' = post-fault EMF of the generator

X_d = direct axis reactance

X'_d = transient direct axis reactance

Thus using this equation in a numerical example (typical case) as cited in reference [34] page 489, P_g was found to be the following

$$P_g \text{ (transient)} = 1.24 \sin \delta - 0.13 \sin 2\delta$$

$$P_g \text{ (steady state)} = 1.50 \sin \delta$$

where

$|V^f| = 0.25$ p.u. $\quad |E'| = 0.993$ p.u. $\quad |E| = 1.50$ p.u.

$X_d = X_q = 1.0$ p.u. $\quad X'_d = 0.20$ p.u.

These equations are plotted in Fig. 2-1. Thus for this typical case, the sin 2δ term has only a second order effect. Therefore typically it can be neglected altogether.

Since for both the transmission line and the generator, the power flow is a sinusoidal function of the phase angle δ, both components can be lumped as a common element between voltage sources. Therefore, when V_a and V_b are referred to in Equation 1, the E' at generator A and generator B will be inferred instead of the voltage at bus A and bus B, with a reactance of

$$X = X_{T\,L} + X_{da} + X_{db}$$

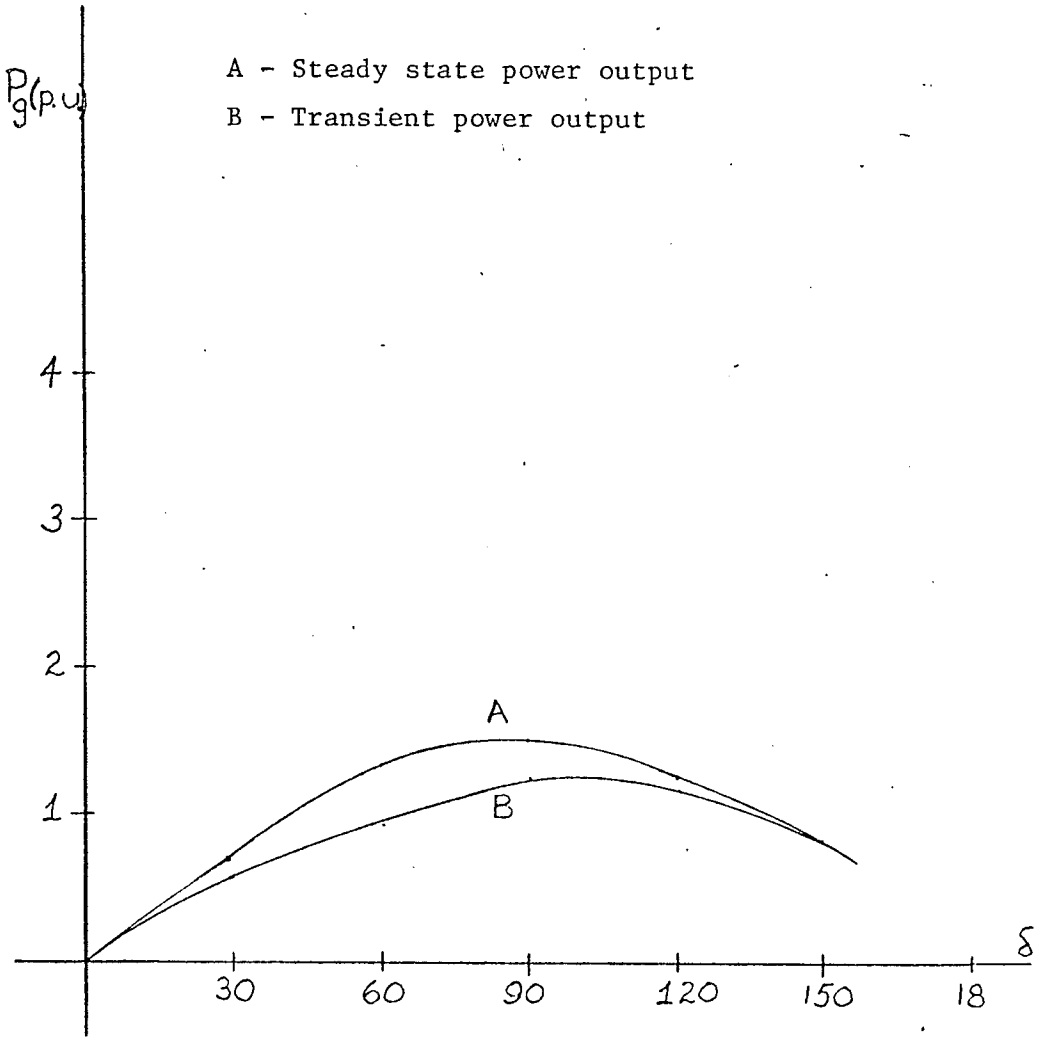

Fig. 2-1: Comparison of steady state and transient generator power output

where

X_{TL} = tie-line reactance

X_{da} = direct axis reactance of generator A

X_{db} = direct axis reactance of generator B

2.3 Effect of Line Resistance on Power Flow Equation

Taking a two area diagram and representing the tie line by a combination of a resistance and an inductance results in the following simplified circuit diagram as illustrated in Fig. 2-2.

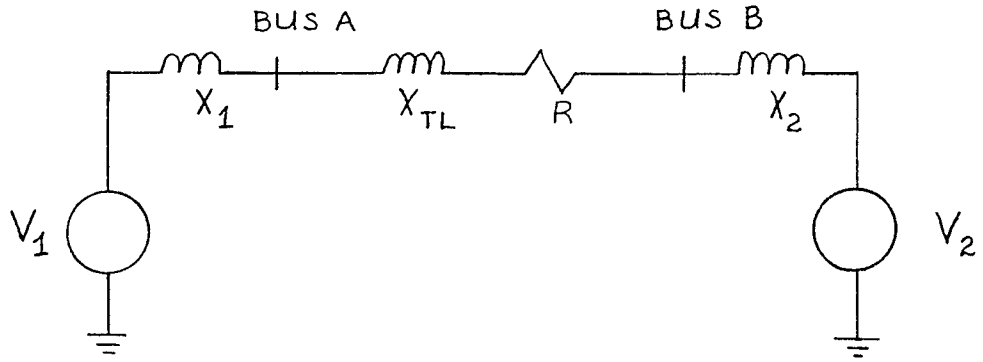

Fig. 2-2 Single Line Diagram

This diagram can further be simplified as in Fig. 2-3.

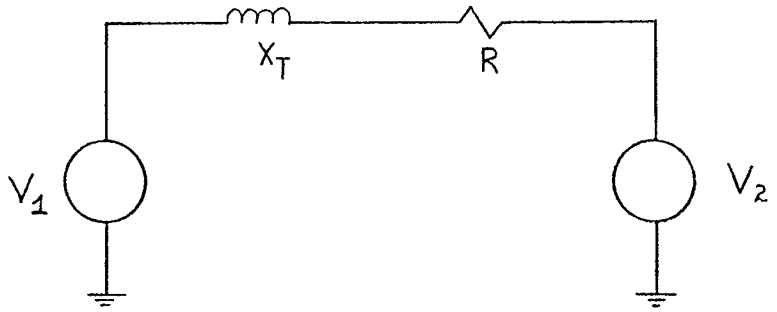

Fig. 2-3 Simplified Single Line Diagram

This problem is analogous to a single transmission link connecting two buses A and B of a large system or two buses of two individual systems. A set of equations for power flowing from one area to the other of this system can then be derived.

The following assumptions can be made:

1) The two bus voltages V_1 and V_2 are known and expressed in phasor values.

2) The link has a series impedance $Z_T = R + jX_T$.

3) The line current is the same throughout the line.

4) Because of losses, the powers measured at the ends of the lines will not be equal. Both power flows S_{ab} and S_{ba} are defined positive directed away from the respective buses.

$$S_{ab} = P_{ab} + jQ_{ab} = V_a I_a^* = V_a \left(\frac{V_a^* - V_b^*}{Z_t} \right) \tag{7}$$

$$= \frac{|V_a|^2}{Z_t} - \frac{|V_a|\ |V_b|}{Z^*} [\cos \delta_{ab} + j \sin \delta_{ab}] \tag{8}$$

where $\delta_{ab} = \delta_a - \delta_b$ = (angle of V_a) - (angle of V_b)

$$S_{ab} = \frac{|V_a|^2 - |V_a|\ |V_b|\ [\cos \delta_{ab} + j \sin \delta_{ab}]}{R - j X_t} \tag{9}$$

$$= \frac{|V_a|^2 - |V_a|\ |V_b|\ [\cos \delta_{ab} + j \sin \delta_{ab}]}{R^2 + X_t^2} [R + jX_t] \tag{10}$$

After expanding equation 10 and separating into real and imaginary parts the following is arrived at:

$$P_{ab} = \frac{1}{R^2 + X^2} [R |V_a|^2 - R |V_a| |V_b| \cos \delta_{ab} + X |V_a| |V_b| \sin \delta_{ab}] \quad (11)$$

$$Q_{ab} = \frac{1}{R^2 + X^2} [X |V_a|^2 - X |V_a| |V_b| \cos \delta_{ab} - R |V_a| |V_b| \sin \delta_{ab}] \quad (12)$$

$$P_{ba} = \frac{1}{R^2 + X^2} [R |V_b|^2 - R |V_a| |V_b| \cos \delta_{ab} - X |V_a| |V_b| \sin \delta_{ab}] \quad (13)$$

$$Q_{ba} = \frac{1}{R^2 + X^2} [X |V_b|^2 - X|V_a| |V_b| \cos \delta_{ab} + R |V_a| |V_b| \sin \delta_{ab}] \quad (14)$$

By setting R = 0 as is often assumed, the equation for P_{ab} is identical to equation 1 in Section 2.1 i.e.

$$P_{ab} = P_{ba} = \frac{|V_a| |V_b|}{X} \sin \delta_{ab}$$

This assumption is often valid since in designing the transmission line R is always made as small as possible to minimize the power loss on the transmission line.

The functional behavior of this power flow is illustrated in Fig 2-4 where both the lossy and the lossless cases are plotted against δ_{ab}. For the lossy case probable practical values of X/R = 3.0 and X = 0.1 with $V_a = V_b = 1$ were used. All numerical values used are in per unit (p.u.).

From this graph certain features are apparent:

1) the angle of maximum power in the lossy case is higher (i.e. 18° more) regardless of what the bus voltages at the ends of the line are;

2) the maximum steady state stability limit of lossy lines is greater than that for lossless lines (at least for lines where X/R ratio is fairly high).

Upon examination of Eqn 11 it is found that this expression can be stated in another form

$$P_{ab} = \frac{V_a}{X(1 + \alpha^2)} [V_b (1 + \alpha^2) \sin (\alpha_{ab} - \tan^{-1}\alpha) + \alpha V_a] \quad (16)$$

where $\alpha = R/X$

For $\alpha = 0$ $\qquad P_{ab} = \frac{V_a V_b}{X} \sin \delta_{ab}$

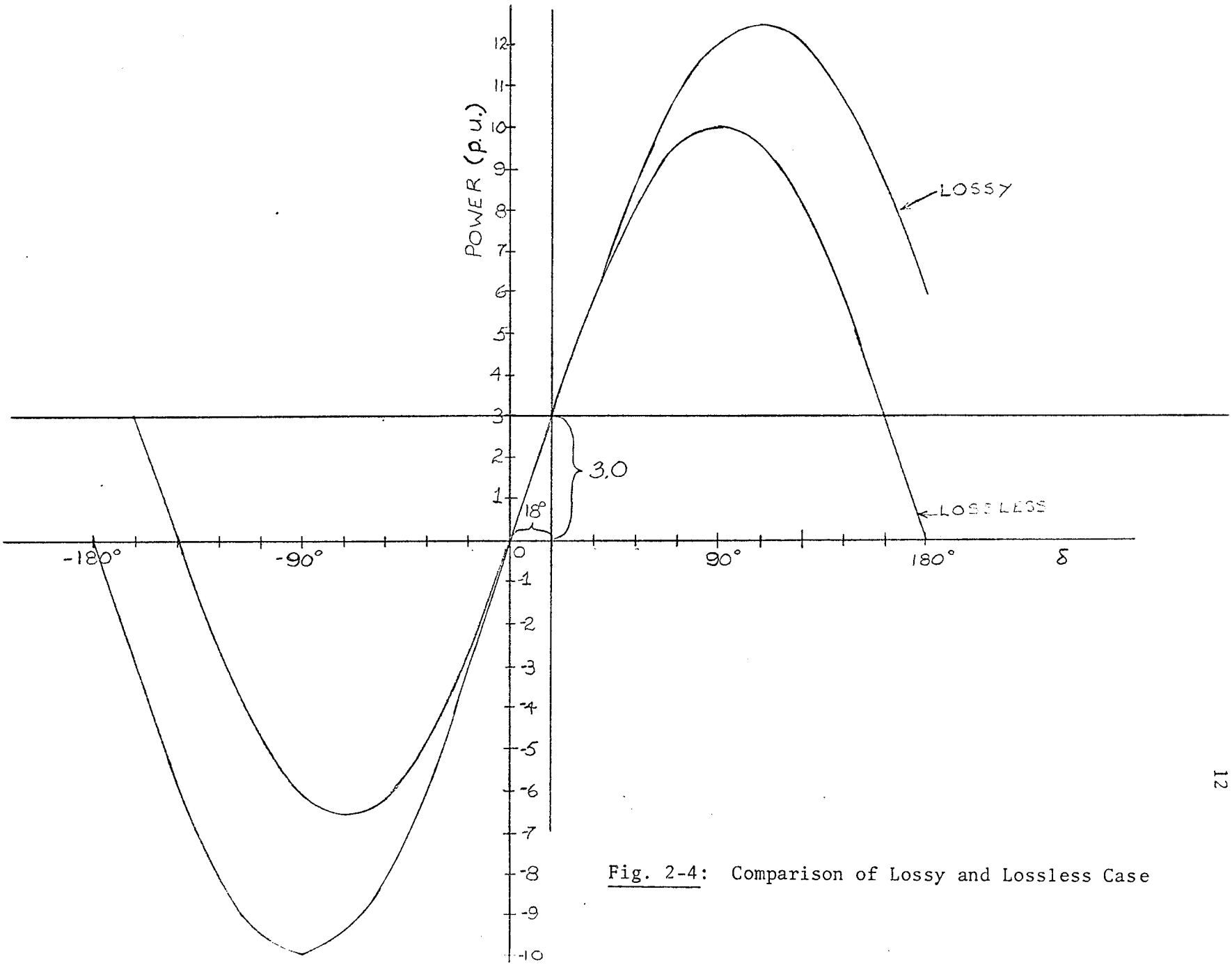

Fig. 2-4: Comparison of Lossy and Lossless Case

Using the same constants used for plotting the graph of Fig 2-4 it can be shown that the expressions for P_{ab} for Eqns 11 and 16 are identical.

Taking the values $V_a = 1.0$, $V_b = 1.0$ and $\alpha = R/X = 0.33$ the following values for Eqn 16 were arrived at:

$$P_{ab} = \frac{1}{0.1(1 + (.33)^2)} [1(1 + .33) \sin (\delta_{ab} - \tan^{-1} 0.33) + 0.33]$$

$$= \frac{1}{.1111} [1.33 \sin (\delta_{ab} - 18.2) + 0.33]$$

$$= 9.0 \quad [1.33 \sin (\delta_{ab} - 18.2) + 0.33]$$

$$= 12.0 \sin (\delta_{ab} - 18.2) + 3.0 \qquad (17)$$

Upon examining Fig 2-4 which was plotted by using Eqn 11 it is found that the curve for the lossy case is described precisely by Eqn 17.

This lossy equation for power represents the power transmitted along the line including both the actual power transmitted to the other end of the line and the power lost in the transmission line due to resistance losses. An exercise illustrating this point is performed in Appendix A.

From this presentation, it is apparent that major swings beyond the operating point (usually around $\delta = 70°$) will enter a region of large power error when resistance is neglected. The amount of error as illustrated in Fig 2-4 is not a true indication of the practical case. Actually $V_a > V_b$ and the resultant curve locus would be below the lossy

case locus in Fig 2-4 where $V_a = V_b$, thus reducing the amount of error encountered.

However the effect of resistance can easily be accounted if desired by introducing:

a) a nonlinearity input offset (e.g. 18.2° for this example),

b) a nonlinearity output offset (e.g. + 3.0 for this example).

These two particular characteristics are illustrated by representing the lossy power flow equation by Eqn 17. For the remainder of this thesis, for reasons of simplification, the used assumption of zero line resistance will be made.

CHAPTER III: THEORY AND DESIGN OF NONLINEARITY

3.1 Theory of Sine Curve Nonlinear Element

In the previous chapter, it was determined that the power flow along a transmission line between points "a" and "b" is

$$P_{ab} = \frac{V_a V_b}{X} \sin \delta_{ab}$$

if the transmission system is assumed to be lossless. This power expression is a constraint, which provides an upper bound to the stable operation of the system. When used for studying transient system behavior this equation introduces a non-linearity into the mathematical model. In this instance, the traditionally available tools of analysis (i.e. root locus, nyquist plots) are unworkable and approximate methods which are not discussed here have to be used. Also for the purpose of analog computer system modelling, the task of representing this non-linearity becomes quite formidable.

A common appraoch used to attack this problem is that of linearization. With this technique, it is assumed that the system operating about a specified operating point between 0° and 45° with small incremental step changes in phase angle δ_{ab} (i.e. in steady state or dynamic stability cases). When the operating point becomes 60° or more or when step changes are quite large (i.e. transient stability cases) operation will occur in the curved area near the peak of the sine wave, and using a straight line approximation does not come near to providing an accurate system representation. Fig 3-1 pictorially illustrates this point.

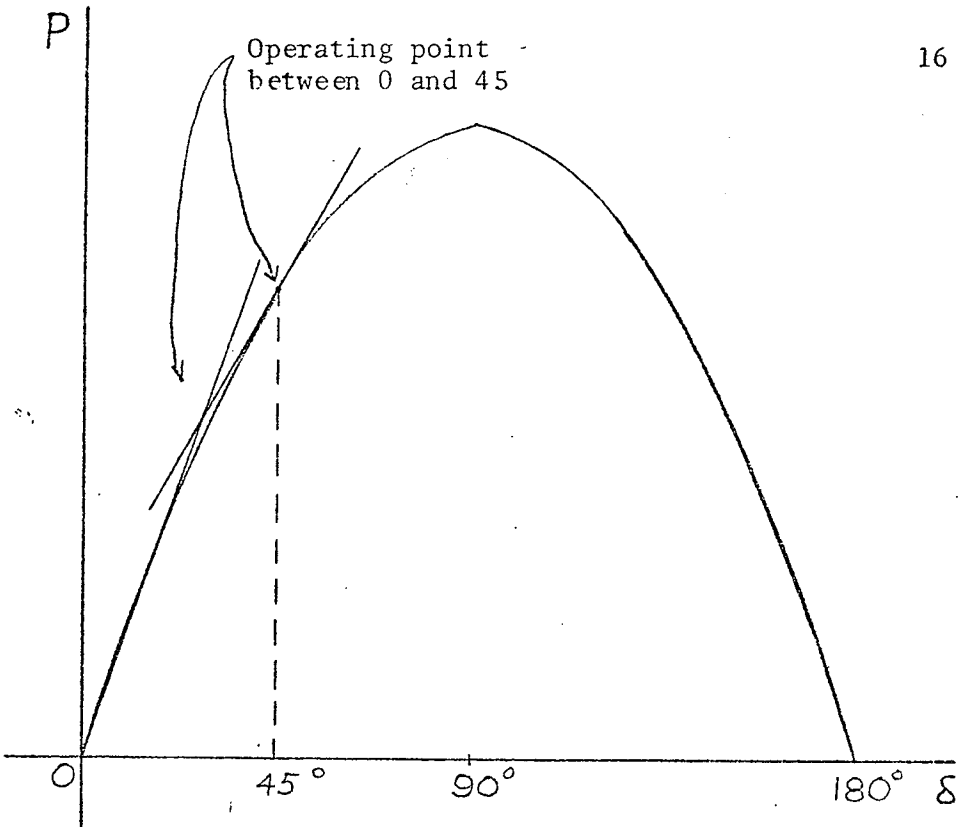

A) Use of straight line segment to represent sine wave power behavior for operating point from 0 to 45

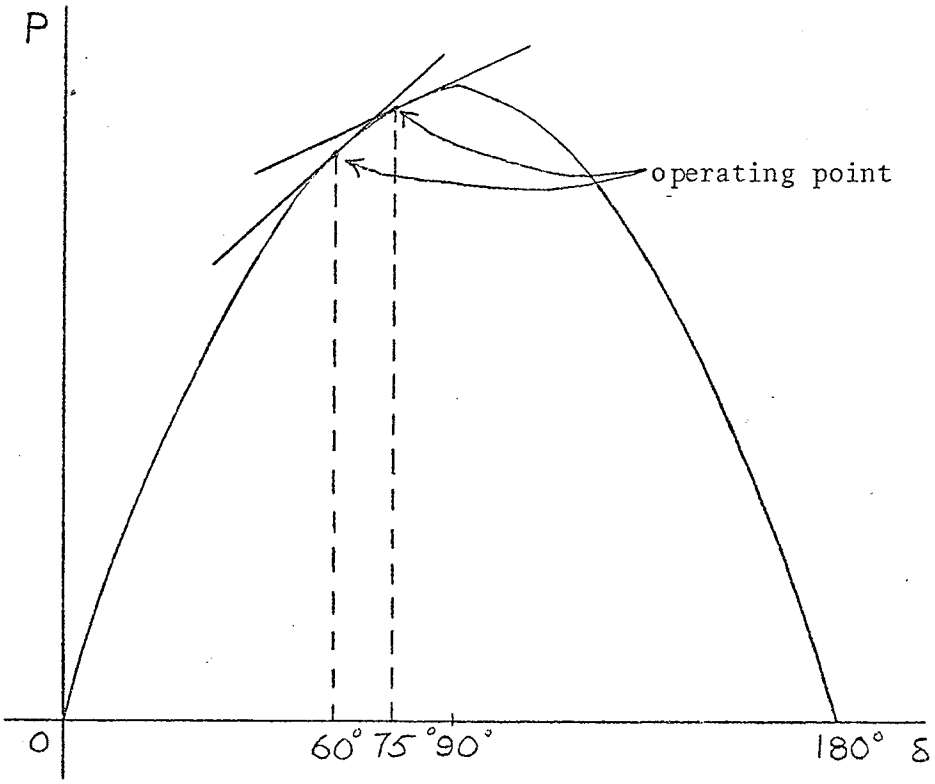

B) Use of straight line segment to represent power flow for operating point 60 and above.

Fig. 3-1: Use of Straight Line Approximations

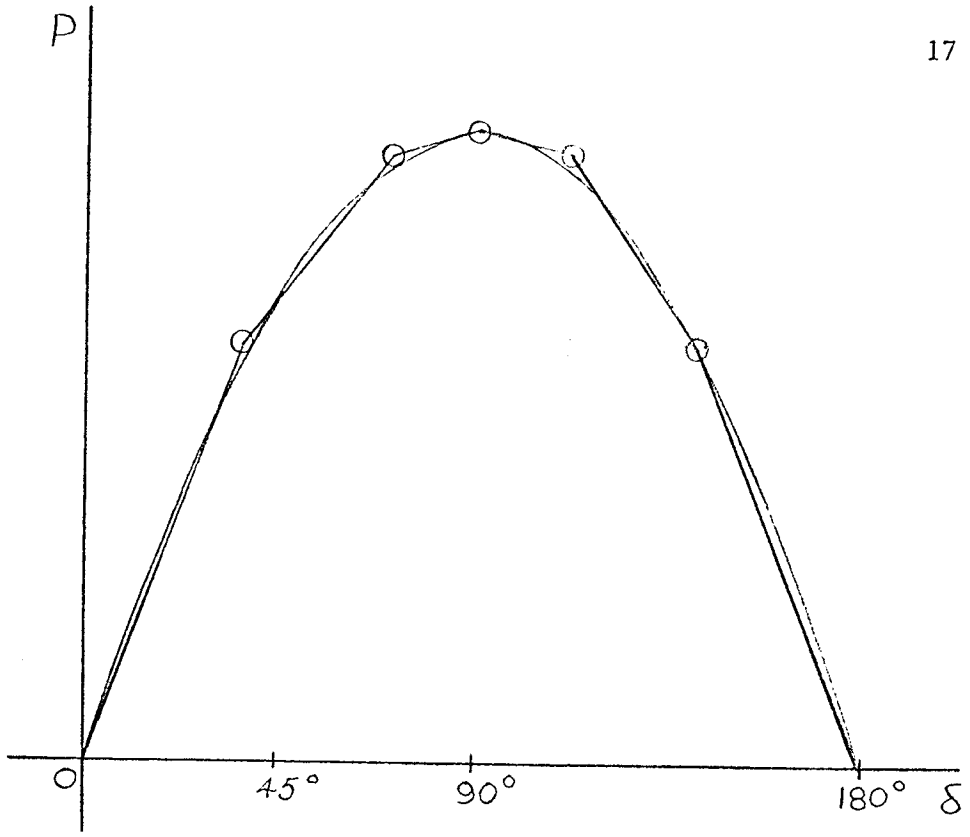

Fig. 3-2: Sine Wave with Straight Line Segments

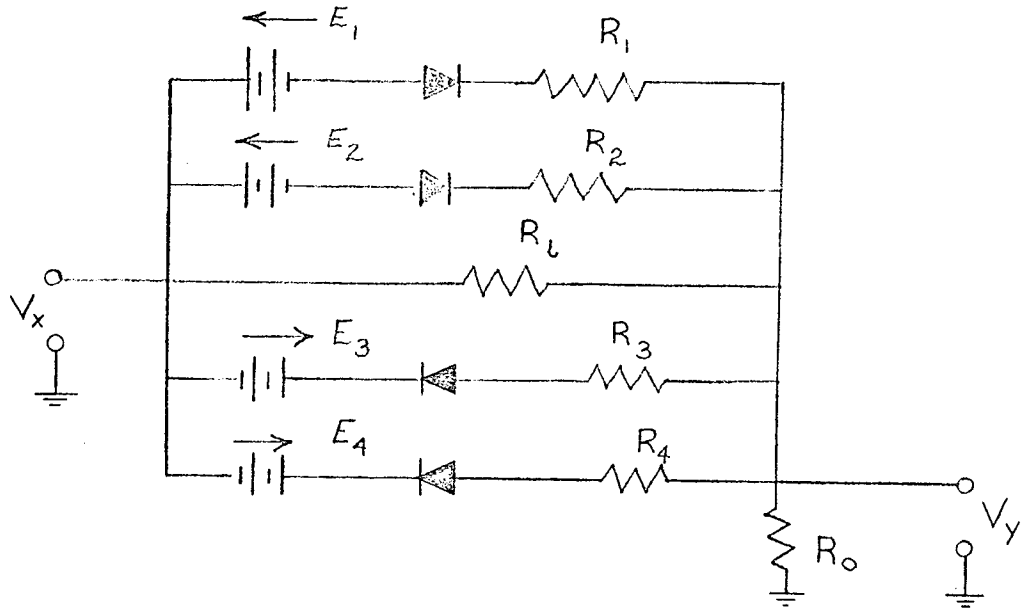

Fig. 3-3: Simplified Functional Diagram of DFG

One part of this investigation consisted of finding a more representative method of simulating the nonlinearity on the analog computer. The approach consisted of representing the sine wave by a group of straight lines, which outline or reasonably approximate the sine wave behavior. This consists in breaking up the sine wave into segments and representing the curved line of each segment by a straight line as illustrated in Fig 3-2.

Different types of configurations exist for accomplishing this piecewise linearization as illustrated in Fig 3-6. General-purpose diode function generators (DFG) afford the ability to approximate nonlinear relationships with a series of straight line segments with adjustable slope and in some versions adjustable segment length as well. Other DFG's have fixed segment lengths. The point where two line segments join is commonly called a breakpoint and the setting up of a DFG involves setting the breakpoints and the sloped of the segments. The diode of the DFG is used as a voltage controlled switch to connect resistances in parallel. Fig. 3-3 is a simplified functional diagram of one of the two basic classes of DFG.

With the voltage representing X at a zero potential, note that the polarity of the battery in series with each diode is such that each diode is back biased, a situation meaning that current cannot flow in that particular branch of the circuit. In this circumstance, the circuit appears as a voltage divider. This results in the following expression relating X and Y

$$Y = \frac{R_0}{R_0 + R_i} X$$

As a matter of fact, as long as the voltage representing the variable X remains less than E_2 or greater than $-E_3$, this relationship is valid.

If however the voltage representing X exceeds E_2 then the diode in series with R_2 is forward biased and conducts which causes R_2 to be connected in parallel with R_i. The relationship between X and Y now becomes

$$Y = \frac{R_0}{R_0 + \frac{R_2 R_i}{R_2 + R_i}} X$$

a relationship obviously different from the previous expression relating X and Y. If the voltage representing X exceeds E_1, then the diode in series with R_1 is forward-biased, as is the diode in series with R_2, and one has resistance R_1, R_2 and R_i connected in parallel causing yet a third different relationship between the voltage representing X and Y.

A similar discussion can be given for the voltage representing X going to negative values. The breakpoints are selected by specifying the voltages E_1, E_2, E_3 and E_4 and the slopes by specifying R_1, R_2, R_3 and R_4. This scheme of DFG illustrated in Figure 3-6(a) suffers from several disadvantages. These are:

1) the nonlinear function must be monotonic

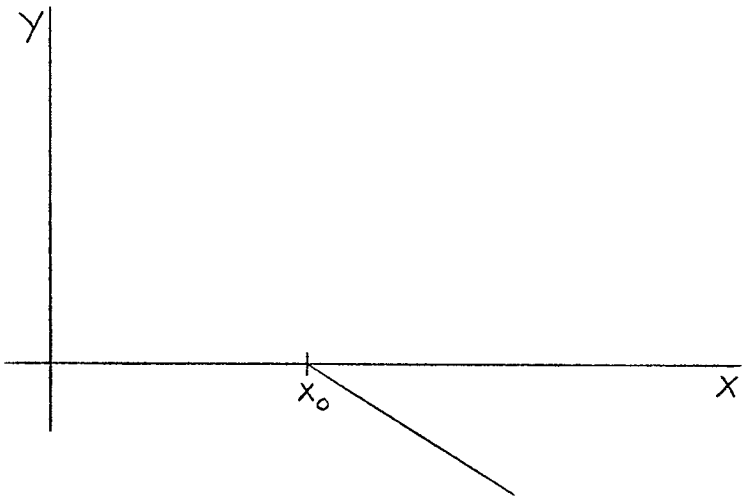

Fig. 3-4: Input Output Relationship of the Circuit of Figure 3-6B

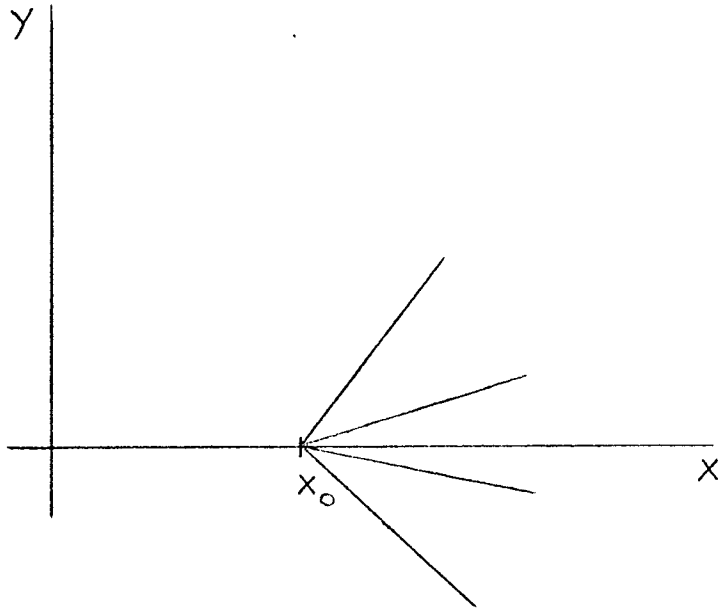

Fig. 3-5: Demonstrates the generation of an Arbitrary Slope by the Circuit of Fig. 3-6C.

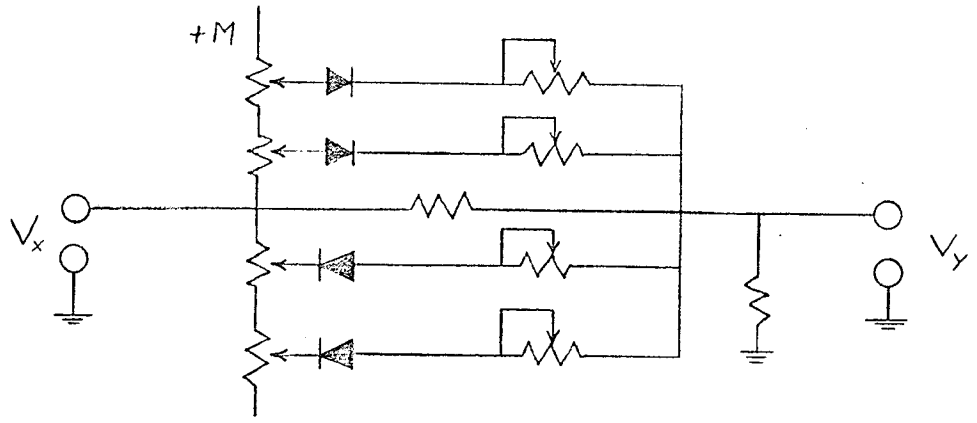

A) monotonic function type diode function generator

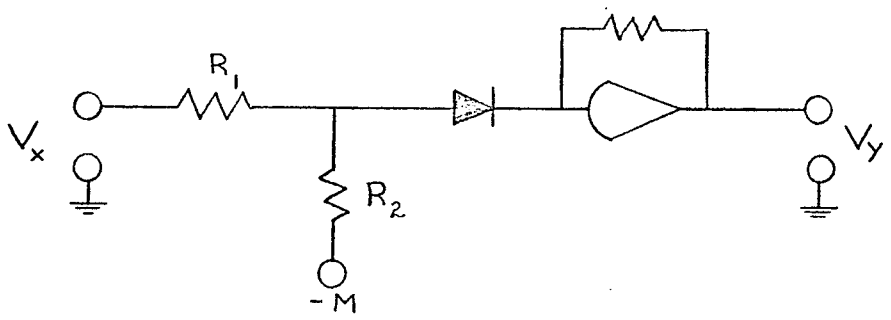

B) circuit to generate a nonlinear function with negative slopes

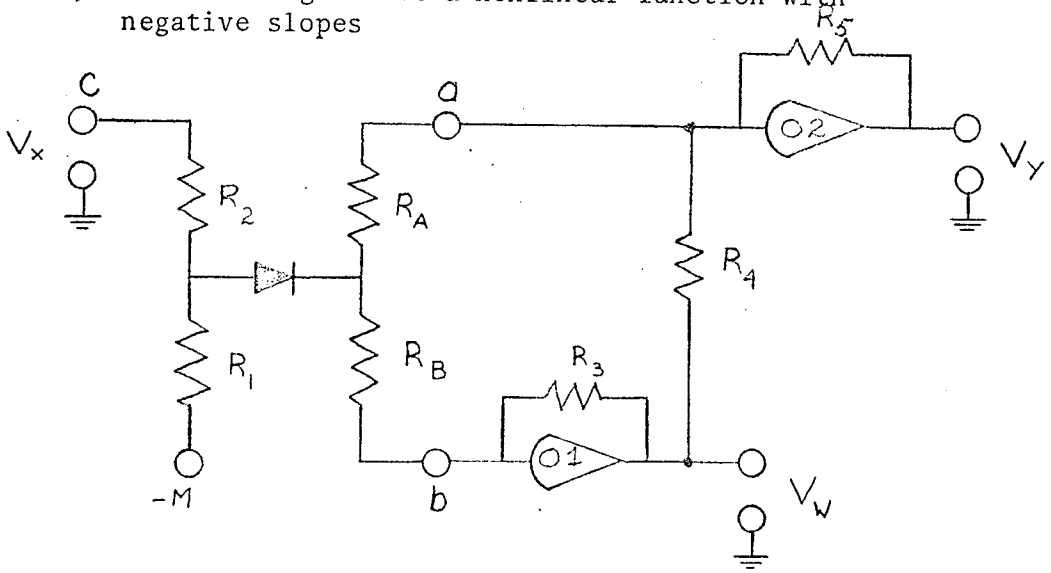

C) non-monotonic diode function generator

M – POWER SUPPLY

Fig: 3-6 Different Types of Diode Function Generators

2) for increasing voltage representing X, the slope of each line segment influences the slope of all the line segments following it. This last disadvantage prevents one from touching up an intermediate slope without having to readjust all succeeding ones.

A second class of DFG is one in which non-monotonic functions can be generated. This class of DFG uses the addition of several nonlinear characteristics. Consider the circuit of Fig 3-6(b). The relationship between the output Y and the input X for this circuit is given in Fig 3-4. The value of voltage at which the breakpoint X_0 occurs depends upon the magnitude of M and the relative sizes of R_1 and R_2. If this relationship is multiplied by a constant, then a slope of practically any value can be obtained for $X > X_0$.

This subtraction can be effected as illustrated in the circuit of Fig 3-6(c). In this circuit R_A acts as an input resistance for the signal from X to amplifier 02, and R_B acts likewise for amplifier 01. Resistance R_4 is the input resistance of amplifier 02 from amplifier 01. The ratio R_5/R_A determines the slope of the characteristic for values of X greater than X_0 at Y, assuming amplifier 01 has been removed from the circuit. This change in slope is the result of the constant multiplier action of the circuit. The ratio R_3/R_B determines the slope of the characteristic for X greater than X_0 at W as influenced by the constant multiplier action. The signal at W is then applied to amplifier 02 through resistor R_4 causing amplifier 02 to function as an adder. Since a sign inversion results from the signal passing through amplifier 01,

in effect a subtraction is occurring at amplifier 02. Thus by controlling the ratio of R_A to R_B, one can establish practically any slope. For negative polarities of X_0, the diode is reversed and a positive fraction of M is applied to R_2.

Additional segments are obtained by repeating that part of the circuit diagram contained between a, b, and c, a suitable number of times and connecting the corresponding terminals of these additional networks to terminals a, b and c. But this class of DFG suffers from the disadvantage that the slope adjustment are dependent upon one another.

The type of DFG best suited for this investigation was the one illustrated in Fig 3-6(c). The reasons for this were

1) the function to be simulated was non-monotonic eliminating use of scheme 1,

2) the requirement of minimum use of operational amplifiers eliminated scheme 2 because there were 11 line segments to contend with, and it would have necessitated 11 operational amplifiers.

Scheme 3 has 11 different line segments yet only uses 2 operational amplifiers.

3-2 Design of the Sine Curve Nonlinearity

Once a suitable circuit has been decided upon, the next problem was that of specifying the design parameters of this circuit. This consisted of the following tasks:

1) determination of the breakpoints and slope values to use in the design of the circuit,

2) determination of the values of resistance to use in the construction of the circuit.

The determination of suitable breakpoint values posed a unique problem because of the infinite combinations possible. The object was to find the breakpoints which would best approximate the sine wave with these linear segments. Theory would dictate that the larger the number of breakpoints used, the more accurate the representation. While in theory this is correct, a practical design must be limited to, say, ten breakpoints. Upon visual examination of a graph of the sine wave, and using a model EAI* 16-304 (+ and -) variable diode function generator, available on the EAI TR-20 analog computer to simulate the sine wave, it was determined that breakpoint intervals of less than 1 volt did not contribute to any significant increase in accuracy. Also in the actual system design, due to tolerances of approximately .2 volts about each breakpoint value, it was found that it would be pointless to specify intervals of less than one volt, because breakpoint values could quite conceivably end up overlapping one another.

A paper from Mathematical Review "Approximation of Curves by Line Segments" by Henry Stone developed an idea for determining the optimum spacing between breakpoints, and the optimum value of slope for least squared error for a specified number of breakpoints. This technique lent itself quite easily to computer optimization solution, and the author stated that a program had been developed to perform this task, but it was not available. Writing such a program was considered beyond the scope of this investigation and therefore a less rigorous method of analysis was settled upon. This consisted of determining visually with

---

* EAI - Electronic Associates' Incorporated

the help of the analog computer VDFG, what the breakpoint values should be and how many of them to include. Once these breakpoints were determined it was then quite easy to perform a least squared error analysis on each segment to determine the optimum value of the slope to use. A program doing just that was written and is illustrated in Appendix B. The circuit set-up used for visual analysis is illustrated in Fig 3-7(a).

Using this experimental set-up, various combinations were simulated on both the analog computer and the least squared error analysis program. The configurations tried are listed in Table I. The ideal set of design parameters was as stated and illustrated in Figure 3-8.

3-3 Building of the Diode Function Generator

As was outlined previously in section 3-1, the circuit of Fig 3-6(c) was chosen. The actual parameter values were established by trial and error methods.

It was decided that the values for M (the diode bias voltage) would be -10 volts for the positive section of the Diode Function Generator and +10 volts for the negative section, since power supplies of (+ or -) 10 volts are readily available on the EAI TR-20 analog computer. This fulfilled the requirement of keeping the amount of equipment external to the analog computer to a minimum, a reasoning which is also applied to other parts of the circuit design.

The next step in the design involved choosing suitable diodes. The kind of diode desired was one with a fairly sharp pickup or switching characteristic to enable the circuit to closely simulate a straight line. A large number of silicon diodes were available from Electrical Engineering

TABLE I

CONFIGURATIONS TESTED TO DETERMINE DESIGN PARAMETERS

TEST CONFIGURATIONS	BREAKPOINTS
1	2.5,4.0,5.0,6.0,7.5
2	2.0,4.0,6.0,8.0
3	2.0,4.5,5.5,8.0
4	2.5,4.5,5.5,7.5

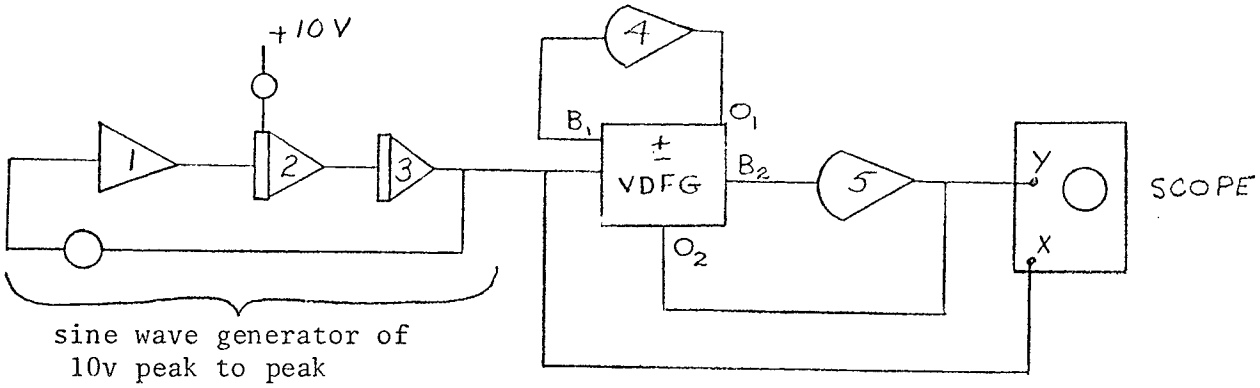

A) circuit used for determining optimum representation

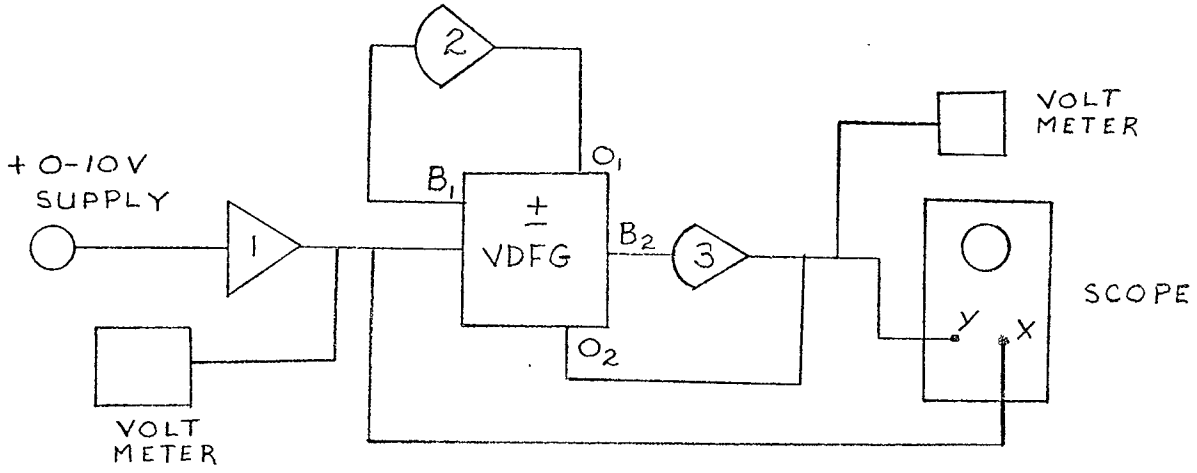

B) Circuit used for detailed determination of slope

Fig: 3-7: Circuits used for Visual Representation

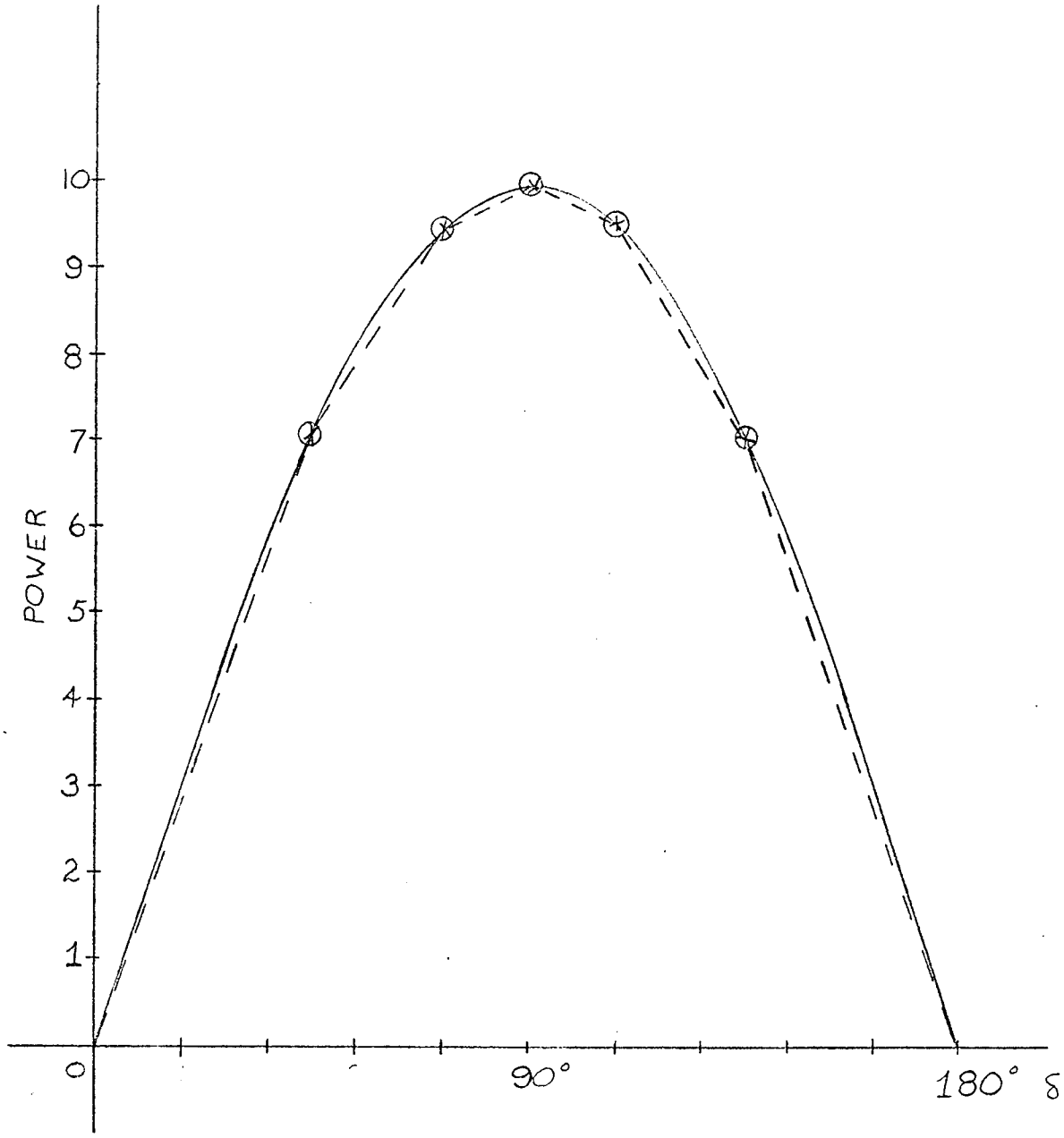

Fig. 3-8: Ideal Line Segments

so they were used. The diodes chosen were ones which had a bias voltage between 0.6 to 0.7 volts, sharp switching characteristics and a linear relationship in the conducting region.

The breakpoint resistances (R_1 and R_2) were the next component values determined. Different values of R_1 and R_2 for each individual segment had to be found. These values were quite easy to determine because the values of resistor used for one breakpoint were totally independent of the values used for a second breakpoint. Once all the appropriate resistor values had been determined by using variable resistance boxes connected to appropriate power supplies, a circuit was connected together.

The next step consisted in finding suitable values for R_a and R_B as well as R_3, R_4, and R_5. The resistor values of R_3 and R_5 were quite easy to determine, and the operational amplifiers of the analog computer were simply connected as adders thus providing feedback resistors R_3 and R_5 of 100K. For R_4 it was decided to use either the 100K adder input resistor or a 10K input resistor. Due to the fact that with the 100K input (adder x 1 mode) the amplifier saturates for an X input of five volts, 10K input (adder x 10 mode) was used. The disadvantage in using this mode of operation was that it caused the DFG to be much more sensitive to temperature changes in the circuit. These resistances R_3, R_4 and R_5 were available within the analog computer and external values did not have to be found. Therefore the actual configuration for the DFG circuit from terminals A-B to the output Y were as shown in Fig 3-9.

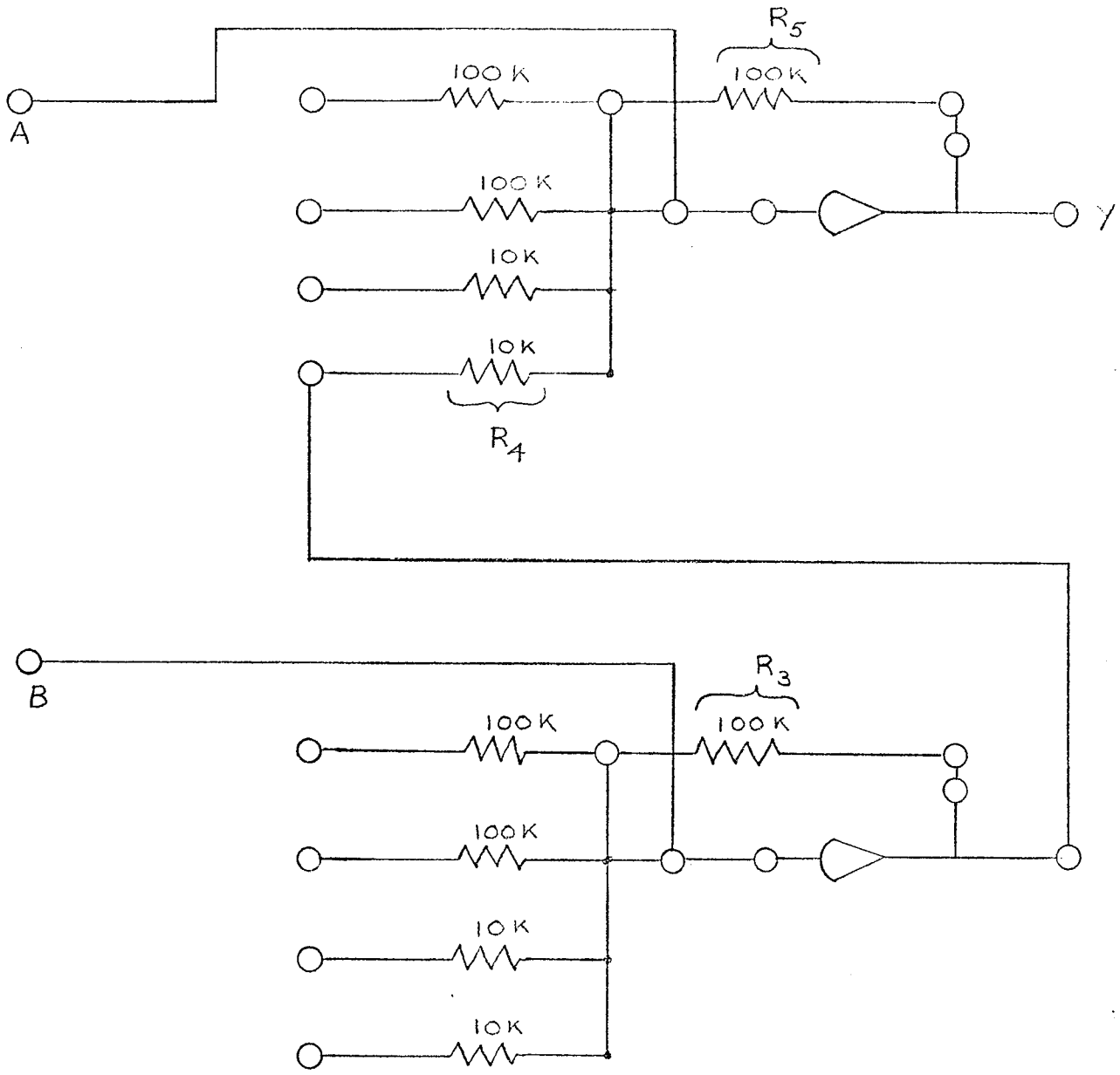

Fig. 3-9: Diagram showing Connections to be made on the Analog Computer

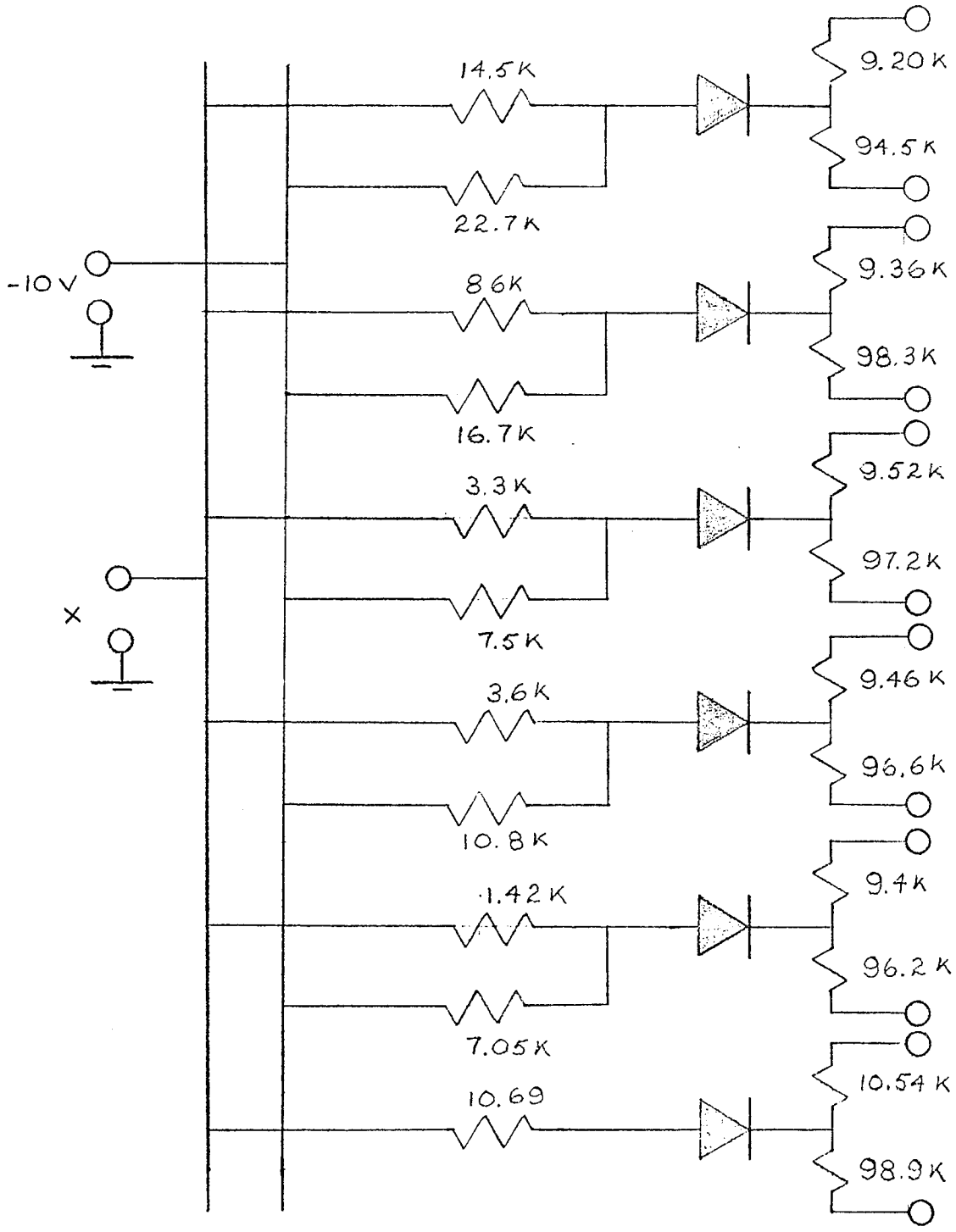

Fig. 3-10A: "+" Diode Function Generator

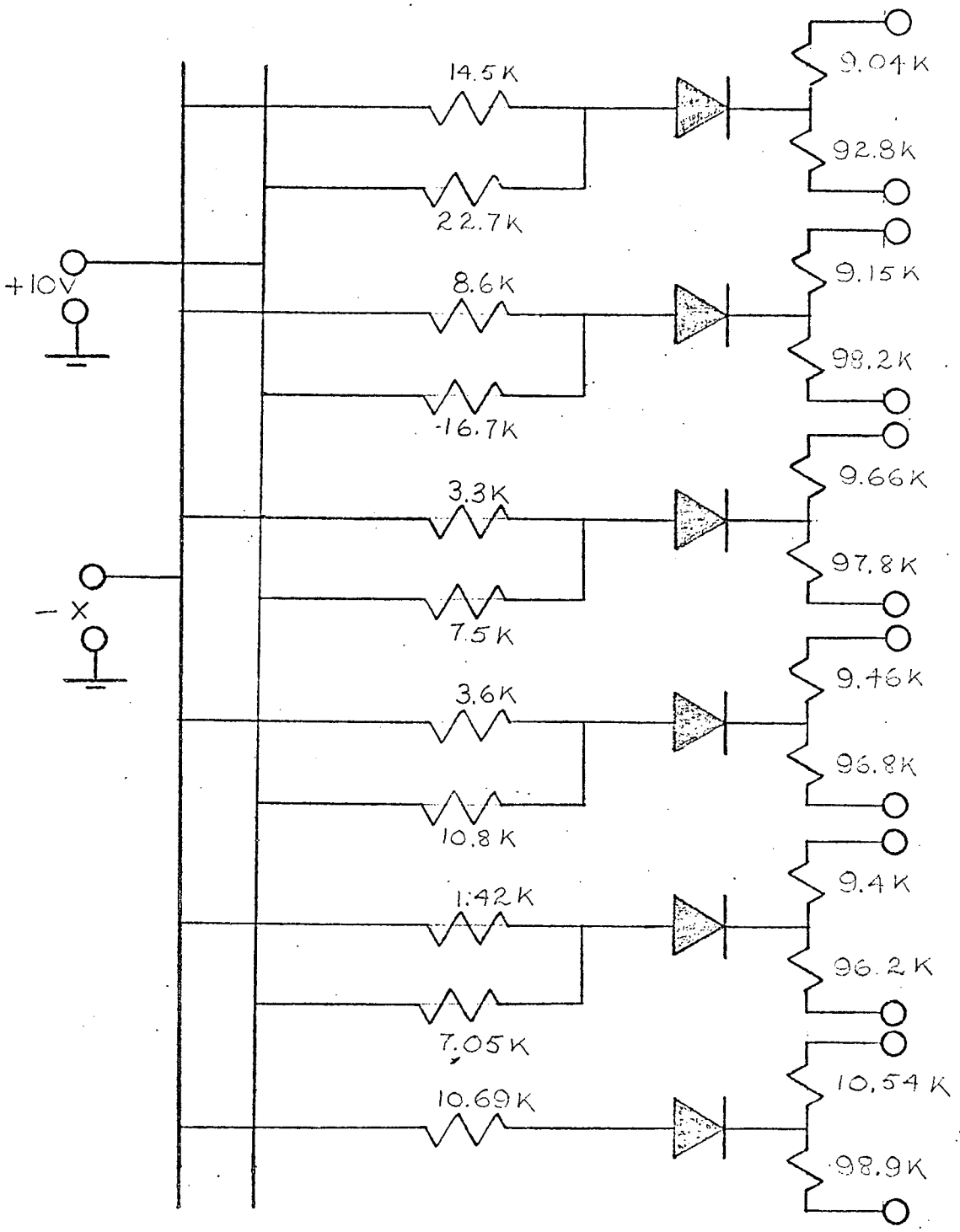

Fig. 3-10B: "-" Diode Function Generator

The final step in this building stage was finding the values of the slope resistances R_b and R_a. The method used was identical to that used for determining the breakpoint values except that the resistor values found were dependent on the values used for the previous segments. This fact made it more difficult to arrive at satisfactory slope values for each segment. The finalized values of R_A, R_B, R_1 and R_2 are shown in Figures 3-10(a) and 3-10(b).

The principle reason for using the two operational amplifiers in their adder mode was that the feedback resistor and input resistor used in an operational amplifier adder mode reduces the requirements for providing resistors and at the same time keeps the number of external connections to a minimum. This has the effect of making the external circuit as simple as possible which satisfies one of the original design criteria established for the circuit.

The tracings of Figures 3.11 illustrates how the circuit so designed simulates a sine wave. As can be seen from these figures the resultant is not a perfect representation of the sine wave but under the circumstances quite satisfactory. The representation behaves basically like a sine wave (i.e. it increases up to a max at 5 volts horizontal representing 90° and then decreases from that point till it reaches 0° at 10 volts or 180°) even though at any particular point the value of the simulation might not be exactly that of a true sine wave. The main thing is that at any particular voltage value the slope of the nonlinearity be in the proper direction (i.e. increasing or positive slope for 0-90° and decreasing or negative slope for 90° to 180°) which is seen to be the case.

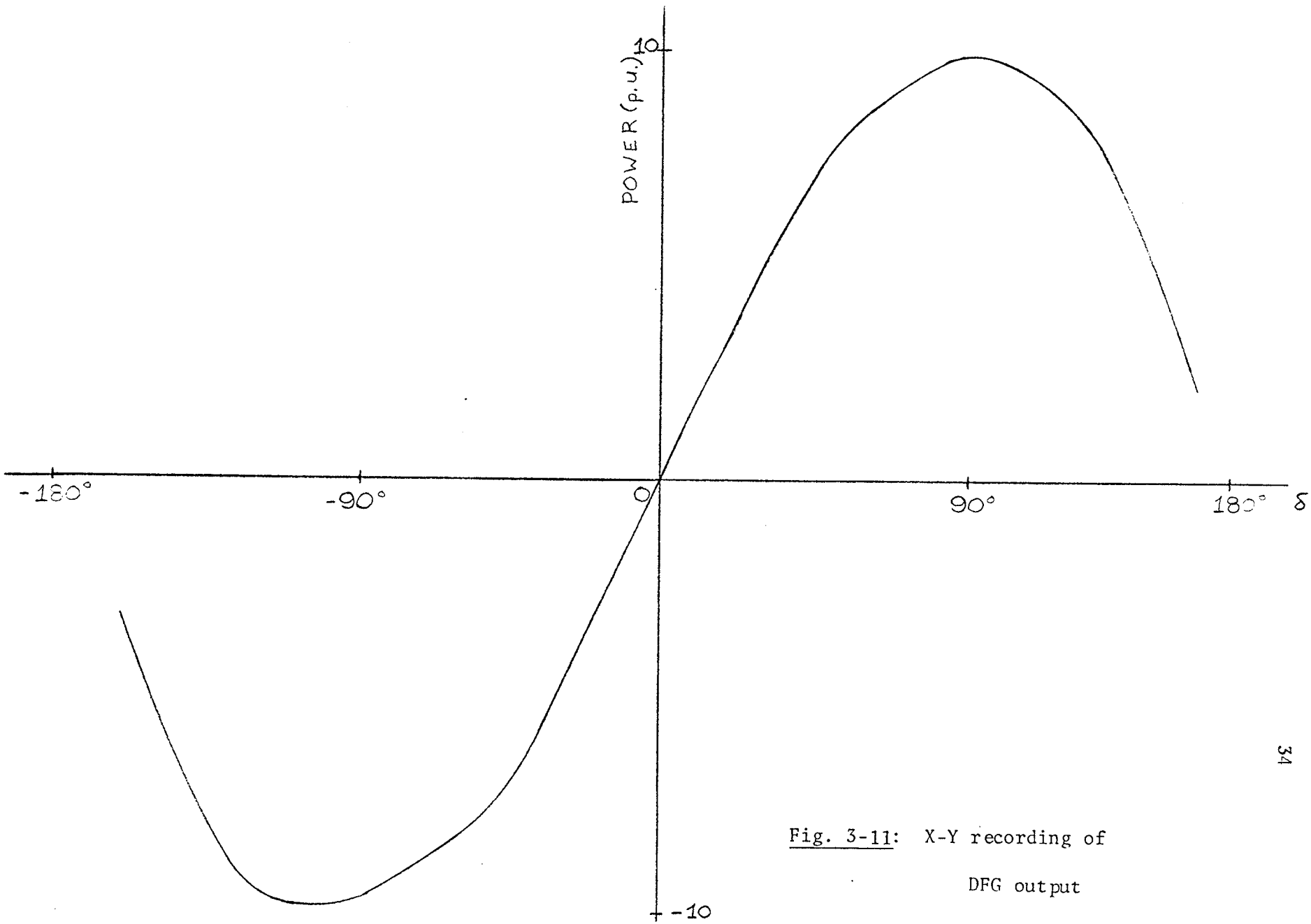

Fig. 3-11: X-Y recording of DFG output

CHAPTER IV: SYSTEM MODELS

4.1 Modelling of the Fundamental Two Bus System

The sine curve nonlinearity must now be tested in an actual system configuration simulation model, i.e. a load and frequency control model. The nonlinearity is an essential part of the load frequency control model, for transient stability studies. This is in contrast to dynamic stability studies for which a linear constant slope behavior about an operating point is appropriate for cases where the system might be operating close to the steady-state stability limit. However, the results obtained from this linear model may be poor.

The block diagram used as the basic representation of a fundamental two bus system is shown in Fig. 4-1. This block diagram representation consists of three blocks representing the system equations. These are:

1) The swing equation of the machine made up of the transfer function relating per unit speed changes to per unit mechanical power changes given by

$$\Delta\omega\ (s) = \frac{\frac{1}{D}}{2\frac{H}{D}s + 1}\ \Delta P(s)$$

where $\Delta P = P_m - P_e$.

Further simplifying this equation the following results

$$\frac{\Delta\omega\ (s)}{\Delta\ P(s)} = \frac{1}{MS + D}$$

where M = 2H = a momentum constant

D = damping constant

H = inertia constant $= \dfrac{231 \times WR^2 \times (RPM)^2 \times 10^{-6}}{(MW)_{base}}$

$$= \frac{\text{megajoules}}{\text{megawatts}}$$

where WR^2 is stored kinetic energy in the rotor

RPM is the revolution per minute of the generator

MW is the system base in electrical power units.

2) A term relating the frequency or speed to the angular displacement . This term enters into the simulation as a term to determine what the angular displacement will be for a specific frequency change.

$$\omega = \frac{d\theta}{dt}$$

$$\text{Therefore } \theta = \int_0^t \omega dt$$

but we are dealing with a change in frequency $\Delta\omega$ so the equation then becomes

$$\Delta\theta = \int_0^t (\Delta\omega)\ dt$$

but $\Delta\theta = \delta$

$$\therefore \qquad \delta = \int_0^t (\Delta\omega)dt$$

In the Laplace domain this equation becomes

$$\delta(s) = \frac{1}{s} \Delta\omega\ (s)$$

thus necessitating a $\frac{1}{s}$ term in the block representation of this system.

3) The third part of the block diagram representation consists of the nonlinearity to determine what the electrical power level is for any value of angular displacement

$$P_e = \frac{V_a V_b}{X} \sin \delta$$

Its reason for being was stated and derived in Chapter 2 of this thesis.

The finalized system model is shown in Fig. 4-1. This is the configuration used for the analog computer studies of the fundamental two bus system or a generator feeding power to an infinite bus. The analog computer patching program used for modelling this system is presented in Fig. 4-2.

This analog computer program was run for different initial operating conditions and step voltages. Three different initial operating points were considered. The meaning of initial operating condition is that point on the P_e vs δ curve that the system is at, when the step disturbance is exerted on the system. Three operating points chosen were 0 volt, 2.5 volt and 4.0 volt corresponding to 0°, 45°, and 72°.

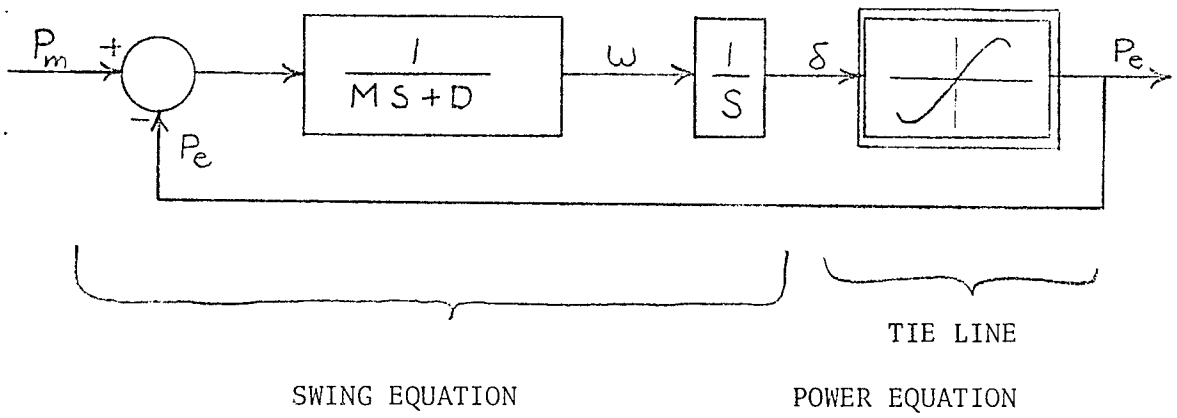

Fig. 4-1: System Block Model

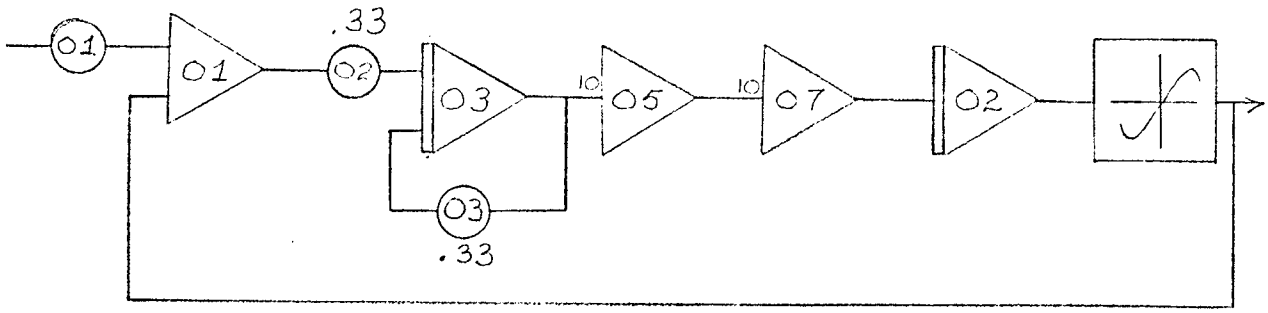

Fig. 4-2: Analog Model of a Two-Bus System

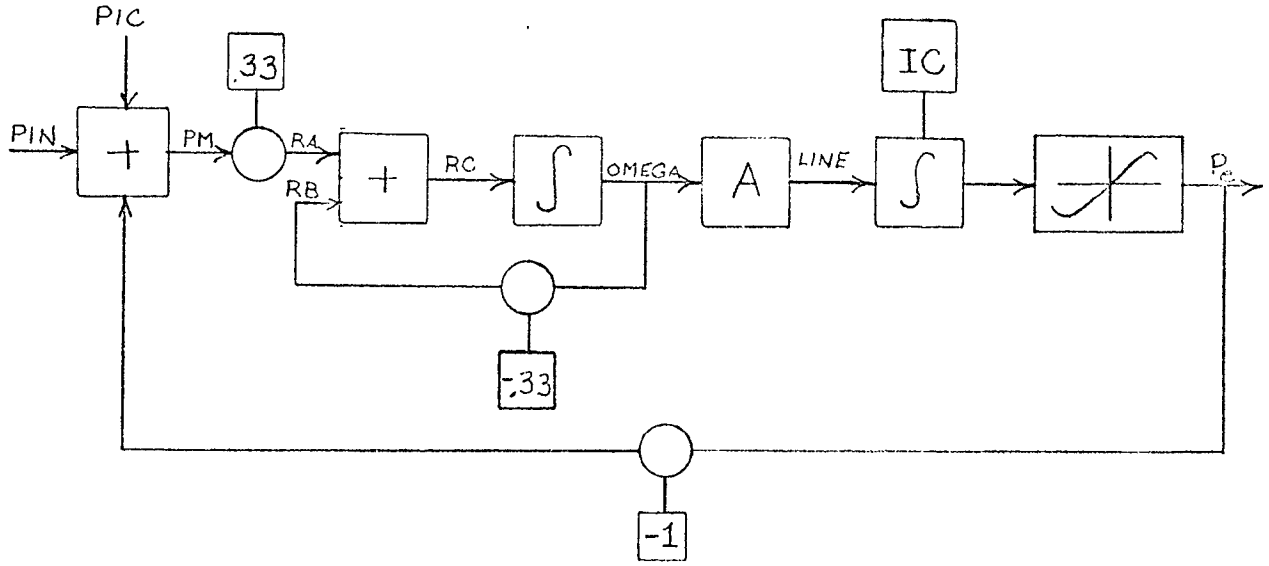

Fig. 4-3: CSMP Model of Two-Bus System

In the model, the values for the parameter constants such as M, D and the constant term in the nonlinearity P_{max} were taken to be the following M = 0.03, D = 0.01 and P_{max} = 10.0. These values are expressed in per unit based on a system base of 100 MVA and are typical.

A series of test runs using a digital computer program called Continuous-System-Modelling-Program (CSMP) was also used to run tests of the model system. The tests here were conducted for the same parameters as the analog system except that the nonlinear function representation was more exact than the one for the analog computer. The block diagram is illustrated in Fig. 4-3 with the program listing shown in Appendix C.

4.2 Addition of Turbine and Governor Dynamics to Fundamental Two Bus System

In section 4.1 a system simulation of a machine or a tightly coupled plant (i.e. acting as a single machine) feeding power to an infinite bus was looked at. In this section, the system is made more realistic by adding governor and turbine dynamics. This system loop can be called the megawatt frequency or pf control channel.

The objective of this control channel is to exert control of frequency and simultaneously of the real power exchange via outgoing lines. This is the problem of controlling the real power output of electrical generators within a prescribed area in response to changes in system frequency and tie line loading, or the relation of these to each other so as to maintain the scheduled system frequency and the established interchange with other areas within predetermined limits.

NON-REHEAT STEAM TURBINE

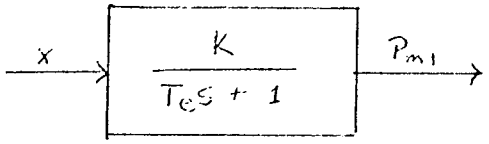

P = turbine power output

X = steam valve opening

T_e = steam starting time determined by volume of entrained steam (seconds)

TURBINE GOVERNOR (speed control mechanism)

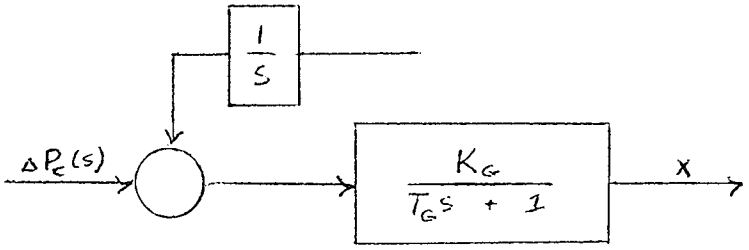

R = speed droop or regulation due to governor action = 0.1

K_g = static gain of speed governing mechanism

T_g = time constant of speed governing system = 0.25

$P_c(s)$ = power increase desired

Fig. 4-4: Model for Governor and Turbine

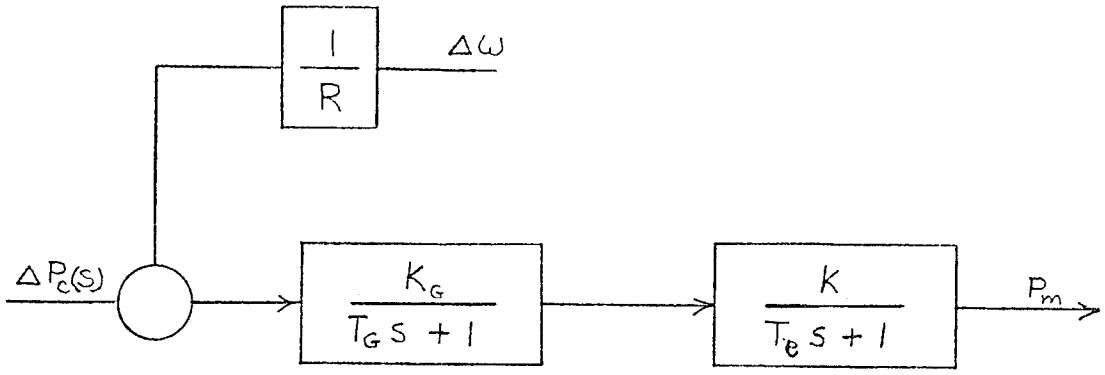

Tg = .10 sec

Te = .10 sec

R = 0.1

Kg = 0.1

K = 0.1

Fig. 4-5: Combination of Governor and Turbine Transfer Function

The control channel consists of a speed governor and a turbine added to the system of part A of this thesis. The mathematical models are derived in Ref. (34) and their block diagram representation is illustrated in Figure 4-4 separately and Figure 4-5 together. The models used were those for the non reheat steam turbine. Other models of turbines (i.e. reheat steam, hydraulic) and governors (mechanical hydraulic, electro-hydraulic, electronic hydraulic) were possible but for the following reasons the non reheat system was chosen.

1) The turbine and governor models chosen were the ones with the simplest mathematical representation.

2) The models chosen required fewer operational amplifiers (which were at a premium on the EAI TR-20) than the other types of governors and turbines.

3) This configuration illustrated the effect of governor and turbine inclusion as well as did the more mathematically complicated kinds.

The complete block diagram is shown in Fig. 4-6.

A group of test runs were made on this particular model using the parameter values as stated in Fig. 4-6 on both the analog computer and the CSMP digital simulation. The analog computer diagram patching program is shown in Fig. 4-7 as well as the digital simulation program listed in Appendix D. The tests were run in a systematic manner similar to those for section 4-1 and the results will be presented and analyzed in the next chapter.

4.3 The Two Area System

In the two previous sections, the simplest of all multi bus systems, the two bus system was dealt with. The load frequency dynamics

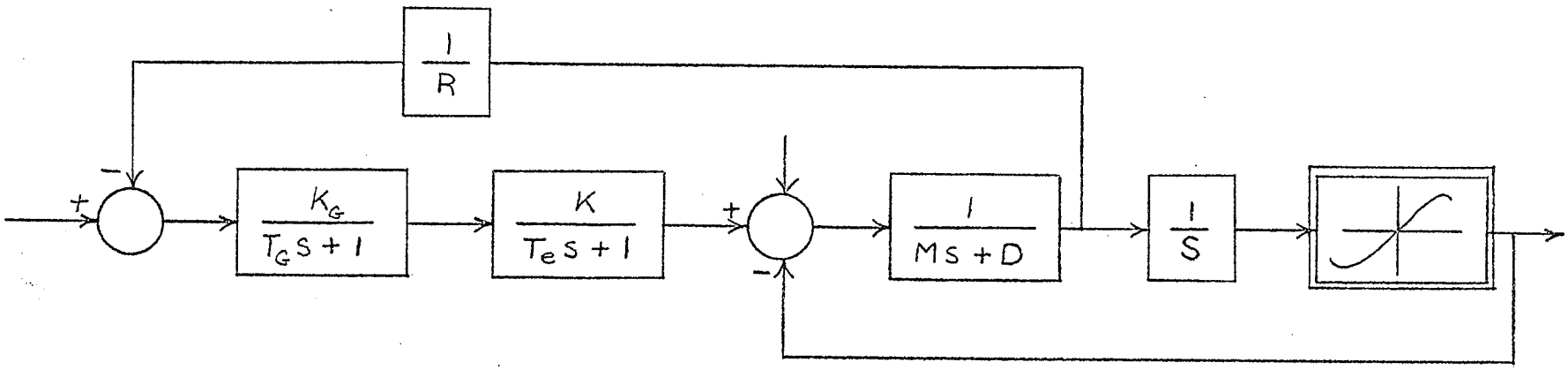

Fig. 4-6: Complete Block Diagram with Turbine and Governor Model Included for the System

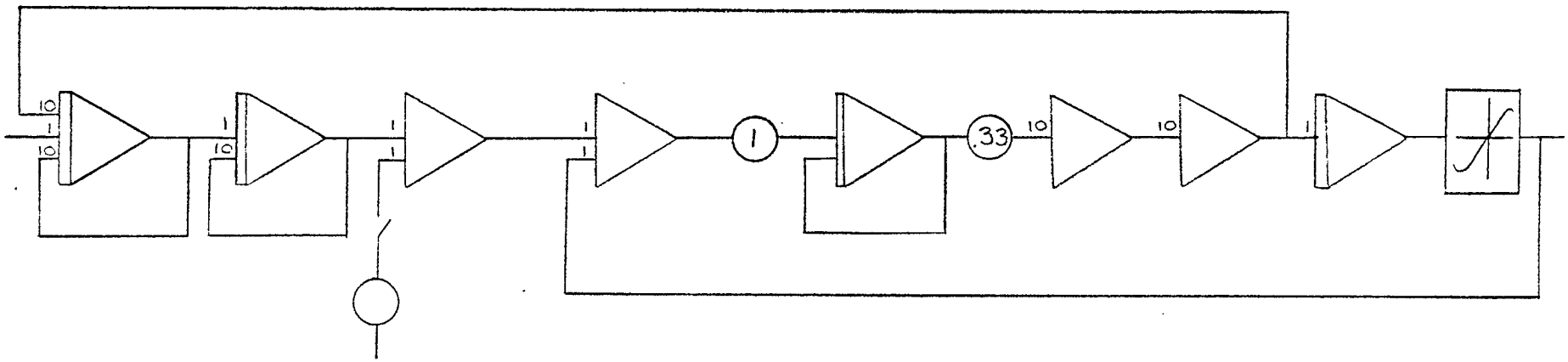

Fig. 4-7: TR-20 Analog Computer Diagram of Model with Turbine and Governor

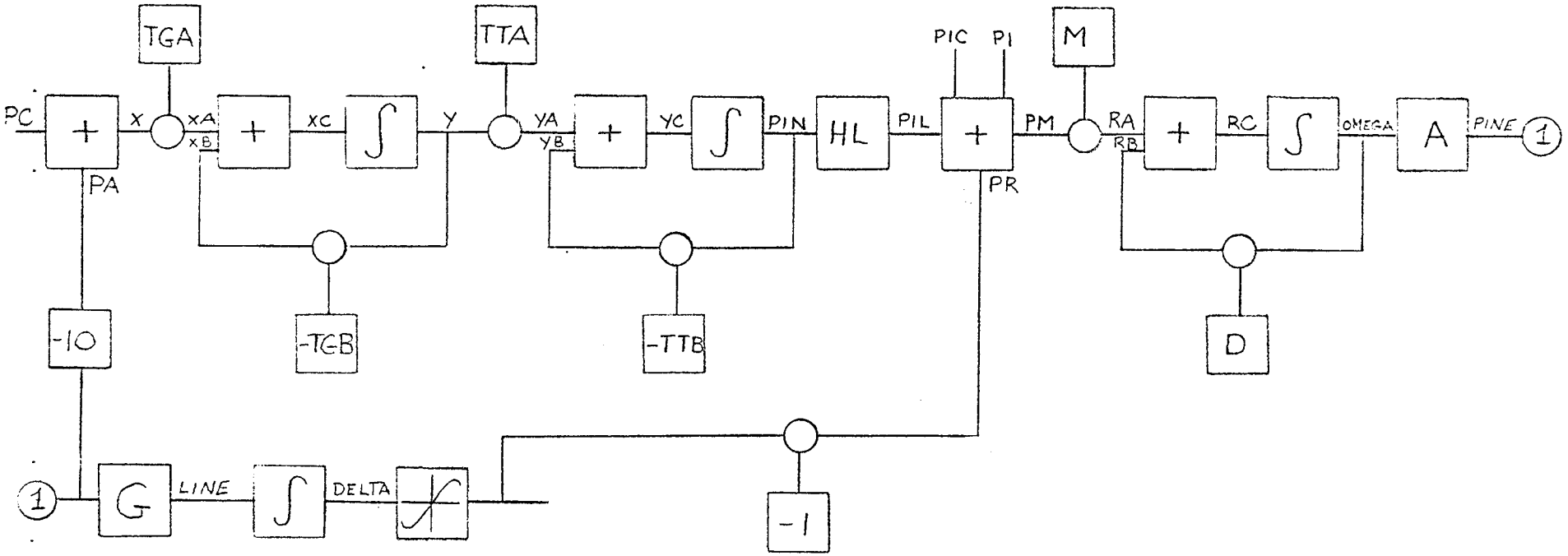

Fig. 4-8: CSMP Diagram of Model with Turbine and Governor

of the n area system are now introduced by considering the dynamics of the two area system.

An area is a part of a system where the machines are tightly coupled together. If a system is made up of two banks of closely coupled machines connected together by relatively weakly coupled transmission lines, we can then represent it as two areas tied together by a tie line as shown in the figure below.

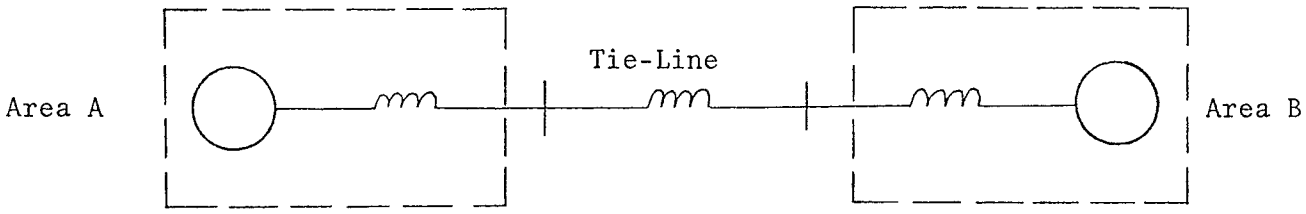

For example either area of the system could have a single line diagram like the following.

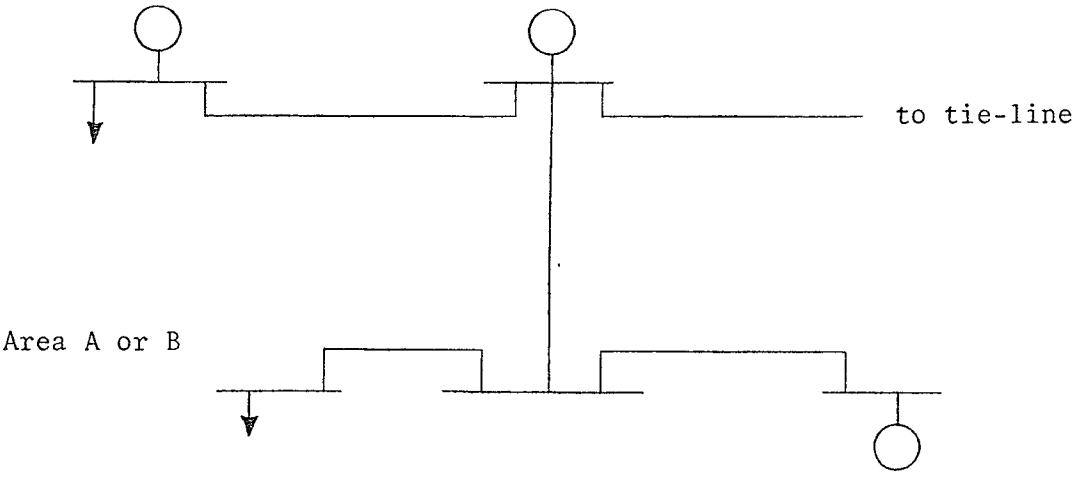

For a power and frequency control loop analysis each area can be characterized by a block diagram similar to Fig. 3-1. Thus for a complete two area system the block diagram would be:

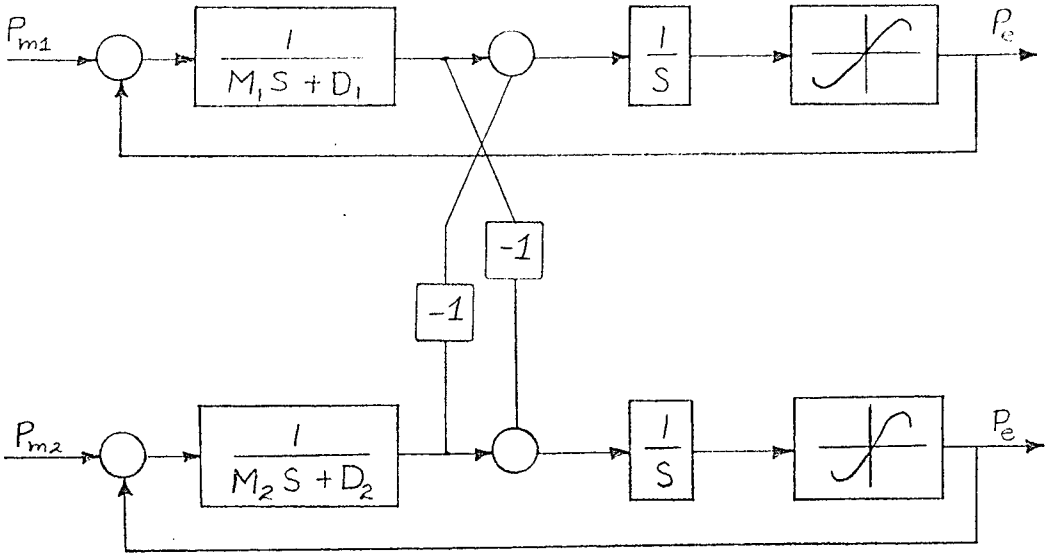

This diagram can then be simplified:

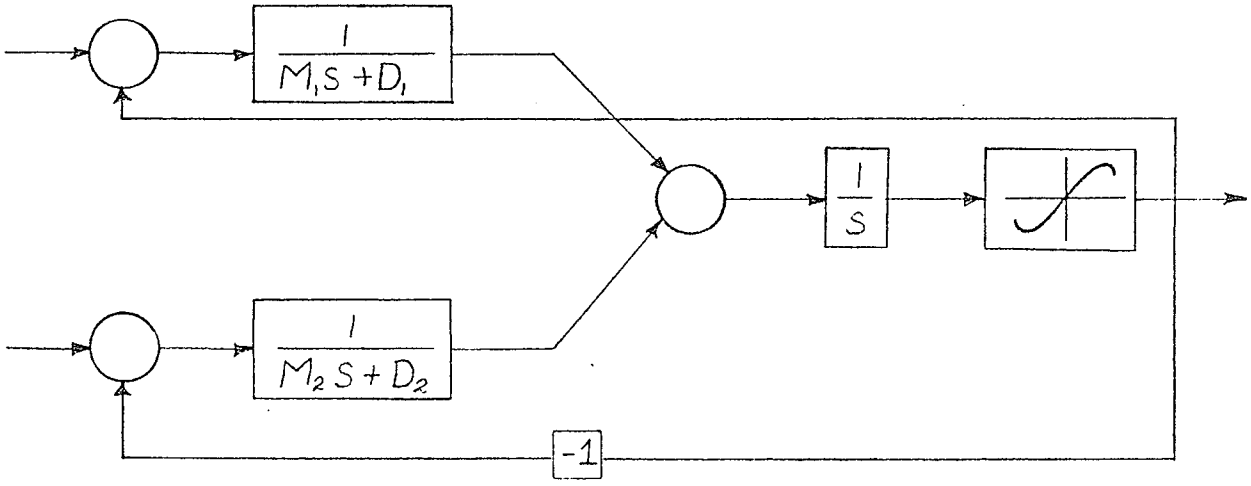

which is the configuration used to study the two-area system.

The analog computer patching diagram for this two area system is as shown in Fig. 4-9.

Tests similar to the two-bus system tests were run on this system. The parameter values in this case were set at $M_1 = 0.03$, $D_1 = 0.03$, $M_2 = 0.0075$ and $D_2 = 0.03$. Tests were again run for the three initial

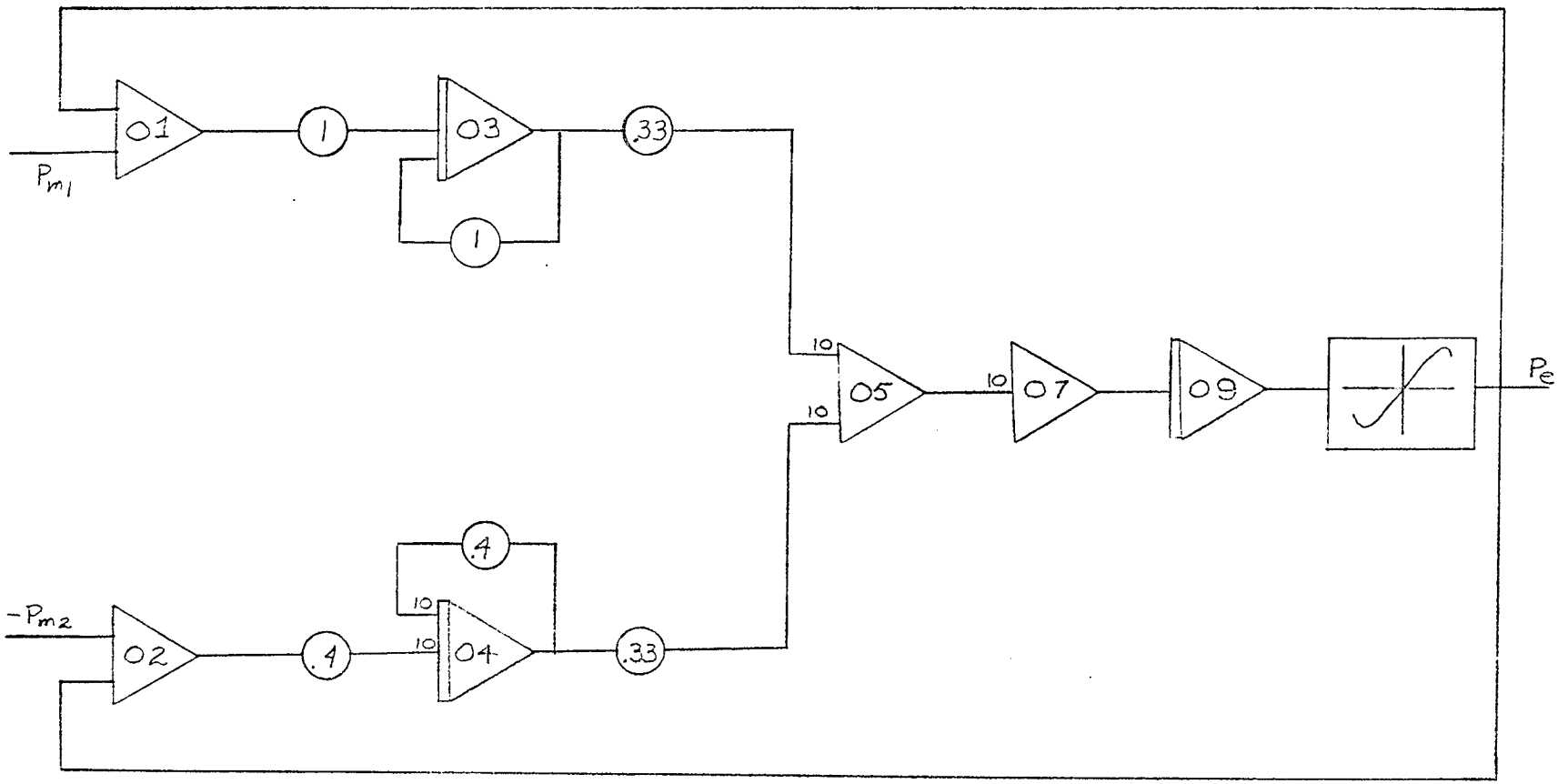

Fig. 4-9: TR-20 Analog Model of Two-Area System

conditions of 0.0 volt, 2.5 volt and 4.0 volts as in the previous set ups. The results will be illustrated and discussed in the following chapter.

CHAPTER 5: PRESENTATION AND COMPARISON OF RESULTS

5.1 Description of Technique used in Running Tests

In the previous chapter, the block diagrams of the system models to be studied were presented along with their equivalent analog and digital patching diagrams. Identical sets of tests were run on each system configuration. A test run consisted of applying a step in P_m to the system model superimposed on initial conditions corresponding to $\delta_0 = 0°$, 45° and 72°.

To determine the degree of accuracy of the model, the step voltage stability limit for each operating point was found. The comparable values of step voltage input stability limit for the analog and digital computer models were determined and discrepancies which arose were explained.

For test series I and II, digital simulations were also run to determine the stability limit using the lossy power angle curve (i.e. with resistance included), to determine a relative figure of error due to the assumption that transmission line was lossless. Similar lossy representation tests were not run on the analog model because of the greater degree of complexity involved in simulating this nonlinearity on the analog machine.

5.2 Results from the Fundamental Two-Bus System

The resultant plots of P_e vs time and δ vs time are illustrated in Fig. 5-1 and 5-2 for the fundamental two bus system. The system step response looks like that of a 3rd or 4th order control system,

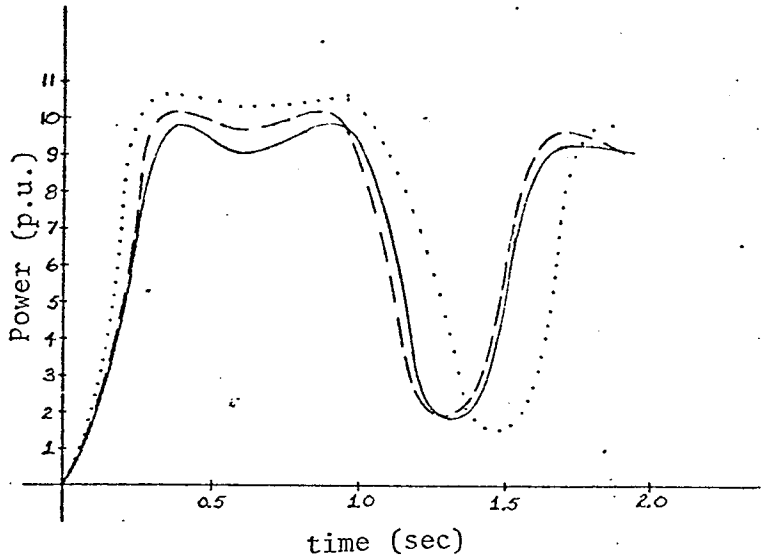

a) initial condition 0^{o}

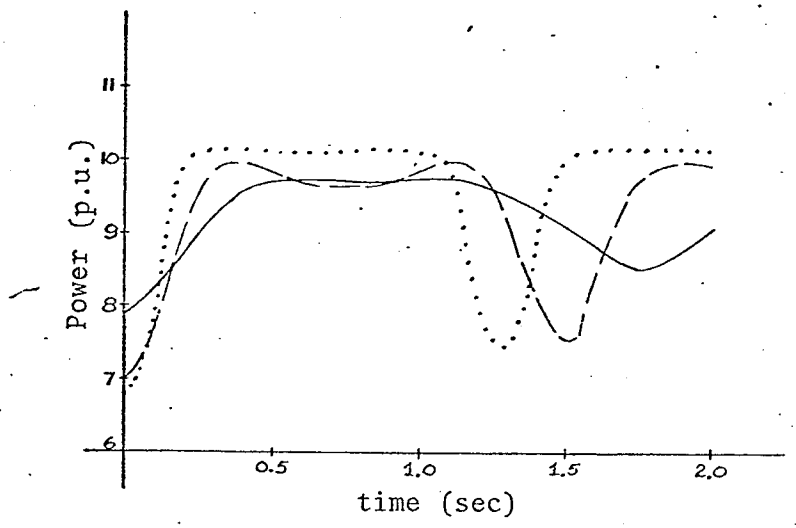

b) initial condition 45^{o}

Digital Lossless Case

Digital Lossy Case

Analog Case

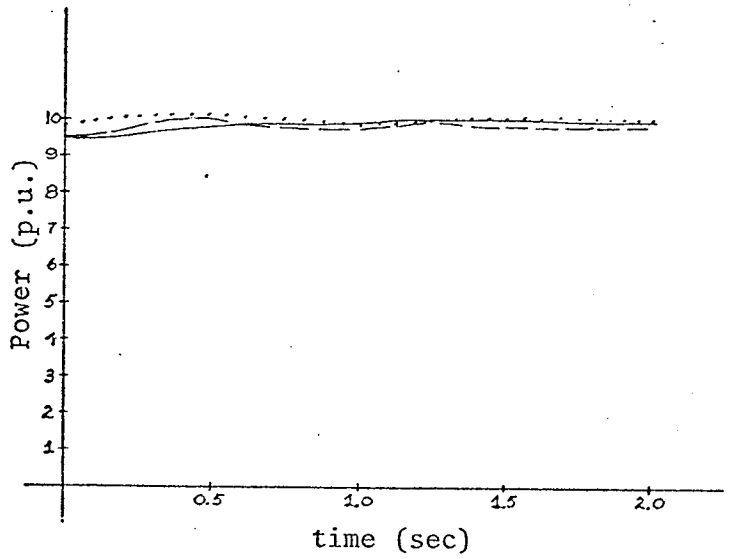

c) initial condition 72^{o}

Fig. 5-1: P_e vs time for Two-Bus Model

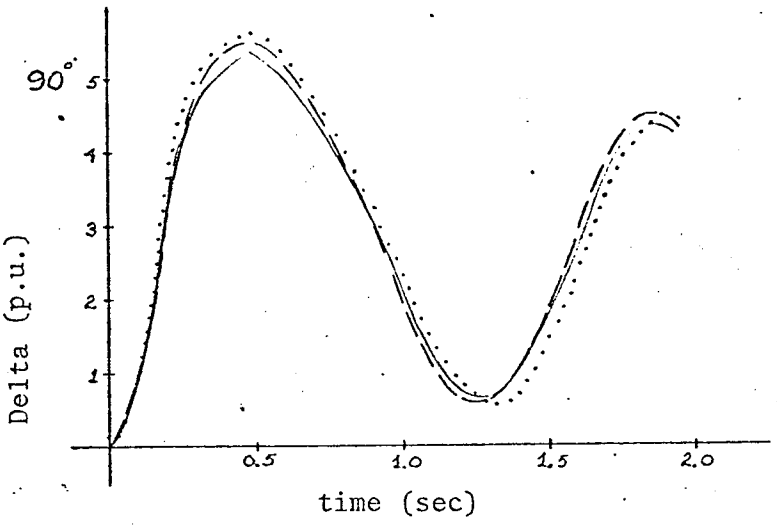

a) initial condition 0^{o}

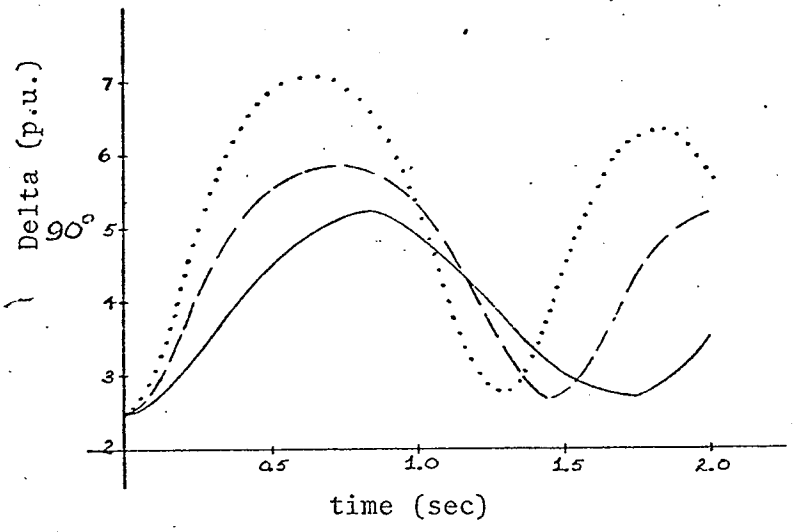

b) initial condition 45^{o}

Digital Lossless Case

Digital Lossy Case

Analog Case

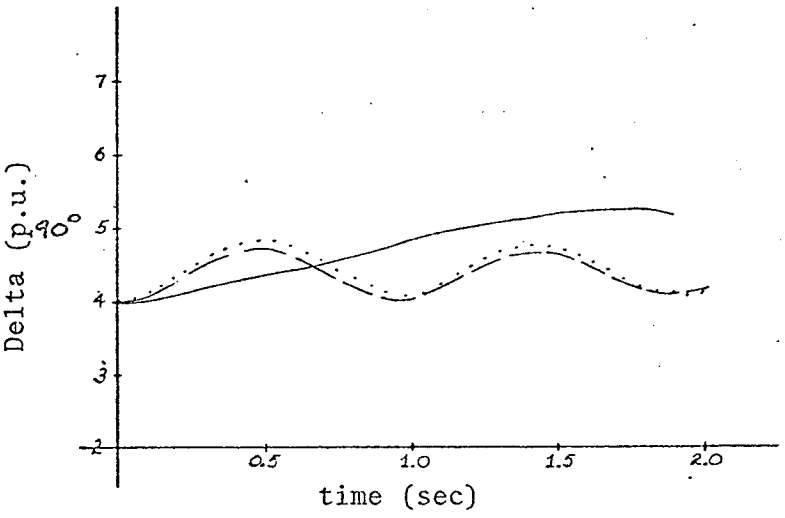

c) initial condition 72^{o}

Fig. 5-2: δ vs time for Two-Bus Model

STEP VOLTAGE INPUT STABILITY LIMIT

Operating Point	Lossy Digital Model	Lossless Digital Model	Analog Model
0.0 volts	8.2 volts	7.3 volts	7.4 volts
2.5 volts	3.4 volts	2.2 volts	1.7 volts
4.0 volts	1.0 volts	.3 volts	.2 volts

TABLE II: List of Step Voltage Stability Limit for Fundamental Two-Bus System.

due to the effect of the nonlinearity, as the plots reveal.

Table II shows a comparison of the step voltage stability limit values between the lossy (resistance included) representation, lossless representation on the digital computer and the lossless representation on the analog computer. The differences in critical step voltage value can be explained by the fact that the sine wave nonlinearity representation on the analog computer was not identical to the digital one. The basis for drawing this conclusion is the equal area criterion explained at length in reference 33. This criterion suggests that the step input stability limit would be different for the digital and analog cases due to the differences in the accuracy of the digital and analog representations of the power-angle curve.

For lossy power angle representation, since the peak is at a larger value of δ, a higher step voltage is required to bring about instability. This agrees with the results of Table II.

For the 0.0 volt operating point test run, a discrepancy seems to occur. The δ term goes beyond 90° on P_e vs δ nonlinearity which should cause the system to become immediately unstable. For transient operating conditions, however, the system can tolerate a δ term greater than 90°. This phenomena can be explained by using the equal area criterion.

5.3 Results for Fundamental Two Bus System with Governor and Turbine Included

The resultant plots of P_e vs time and δ vs time for this second model are presented in Figures 5-3 and 5-4. An examination of these plots reveals that the system is still oscillatory in nature just as in model A. Also, in this model, the damping constant (D) of the system

was increased from 0.01 to 0.03, resulting in a system which damps out to its steady state value faster than does model A.

The amplitude of the oscillations is much smaller than those in the tests of section 5-2 due to the regulating and stabilizing action of the turbine and governor. Due to these two added control elements and the omega feedback loop in the system, the resultant output tends to rise to its new steady state value, overshoot it a bit, oscillate about that point a short while and then settle down. Due to these oscillations being quite small, the step voltage input that the system can tolerate under any initial operating point without going unstable has increased somewhat over the model without turbine and governor.

Upon comparing the digital and analog plots for various operating points it was found that the amplitude of oscillation and the frequency of those oscillations are approximately equal. For example, looking at the δ vs time graph for 0.0 volts operating point, the maximum amplitude for δ is 121.5 degrees in the analog case and 119 degrees in the digital case.

Fig. 5-5 illustrates the system behavior when the step input is so large as to cause instability. An analog trace of P_e vs time and δ vs time is presented in this figure. It is evident that as the step voltage is applied the power increases to the maximum value and then starts decreasing as δ goes beyond 90^o or 5 volts. Once beyond that point, the slope term of the nonlinearity is no longer positive, thus causing the system to possess positive feedback which in turn causes the δ term to start increasing exponentially causing the power term P_e to go to zero. The relatively flat area is due to the slope being so

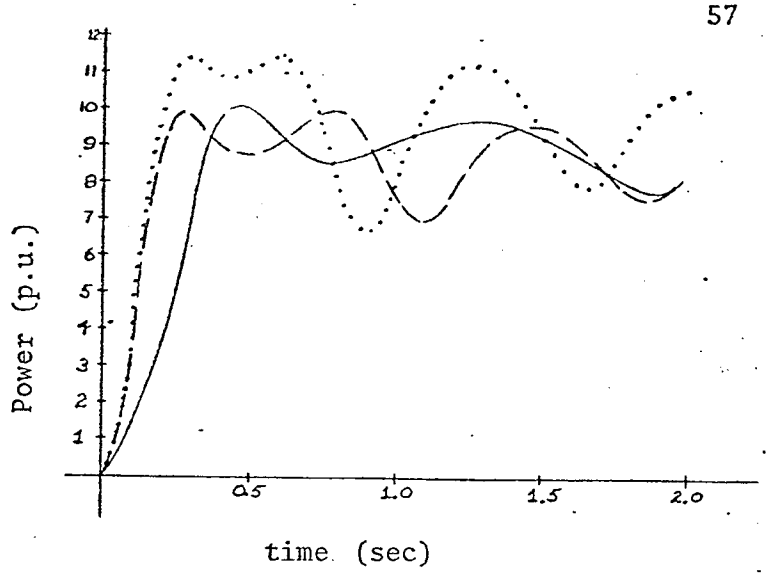

a) initial condition 0°

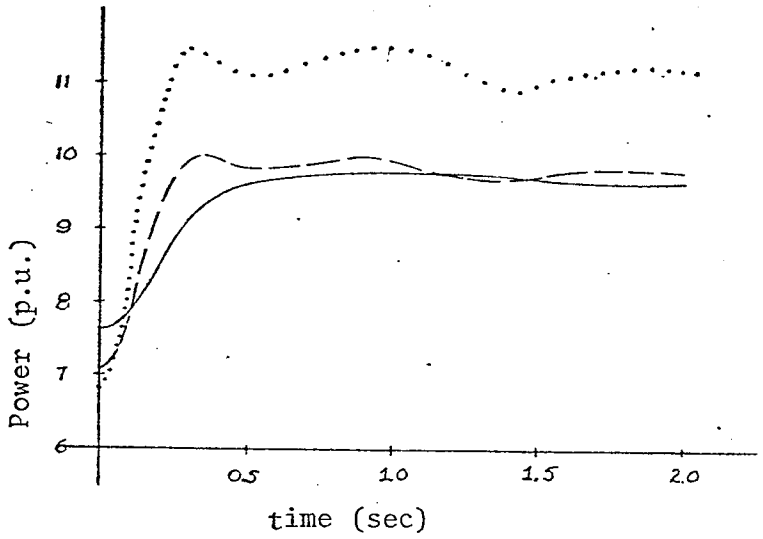

b) initial condition 45°

Digital Lossless Case

Digital Lossy Case

Analogue Case

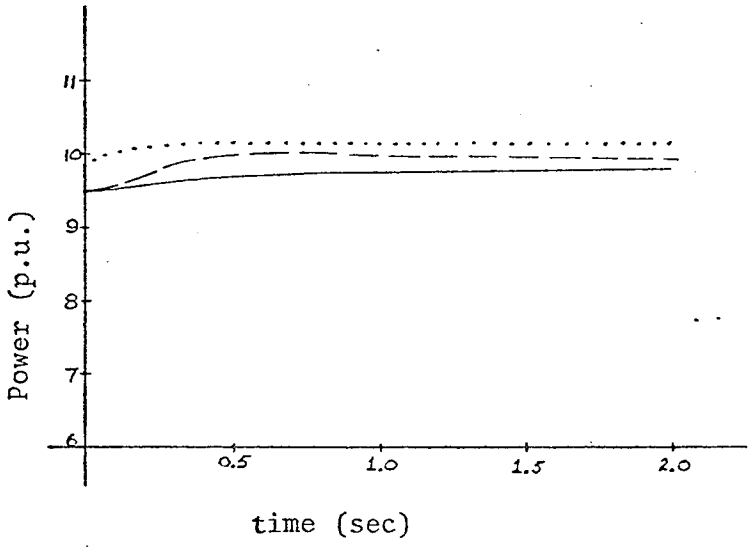

c) initial condition 72°

Fig. 5-3: P_e vs time for Governor and Turbine System Model

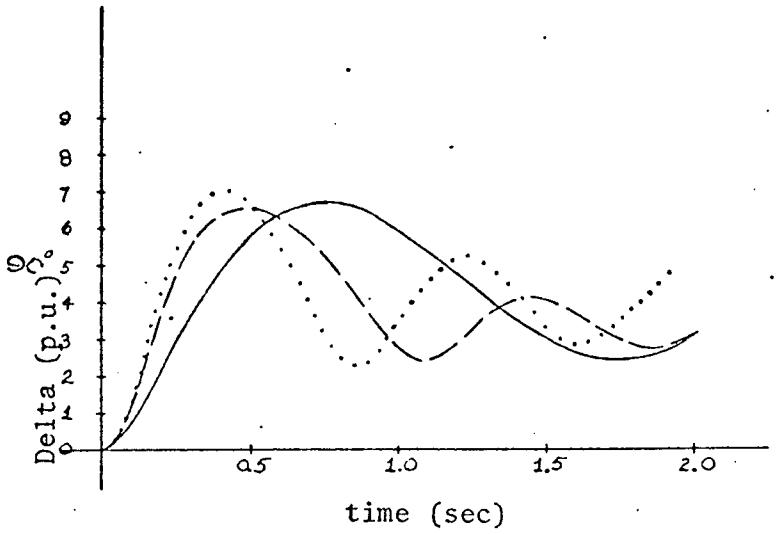

a) initial condition 0^{o}

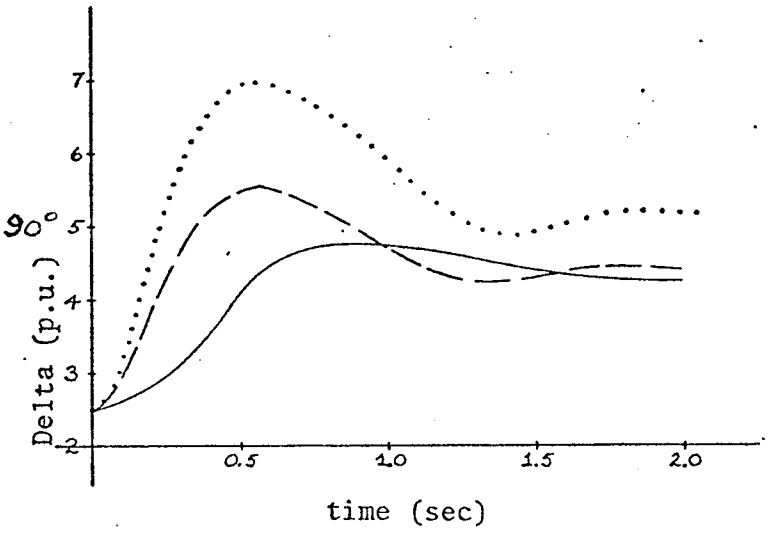

b) initial condition 45^{o}

Digital Lossless Case .....

Digital Lossy Case — — —

Analogue Case _____

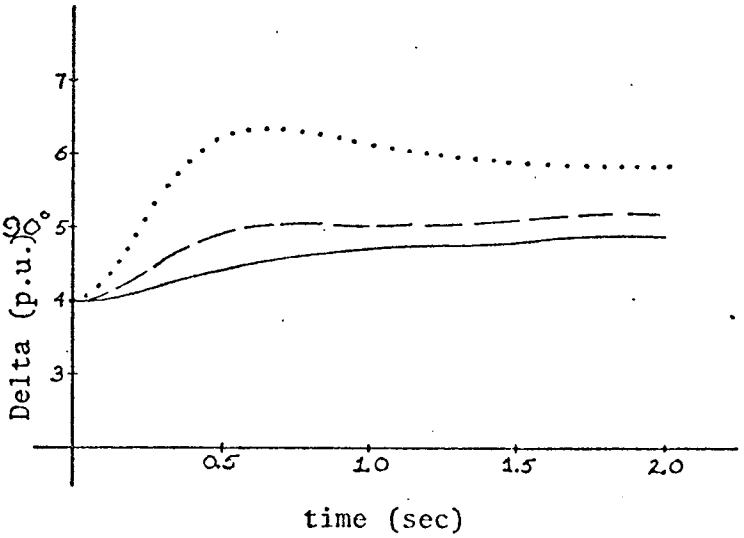

c) initial condition 72^{o}

Fig. 5-4: δ vs time for Governor and Turbine System Model

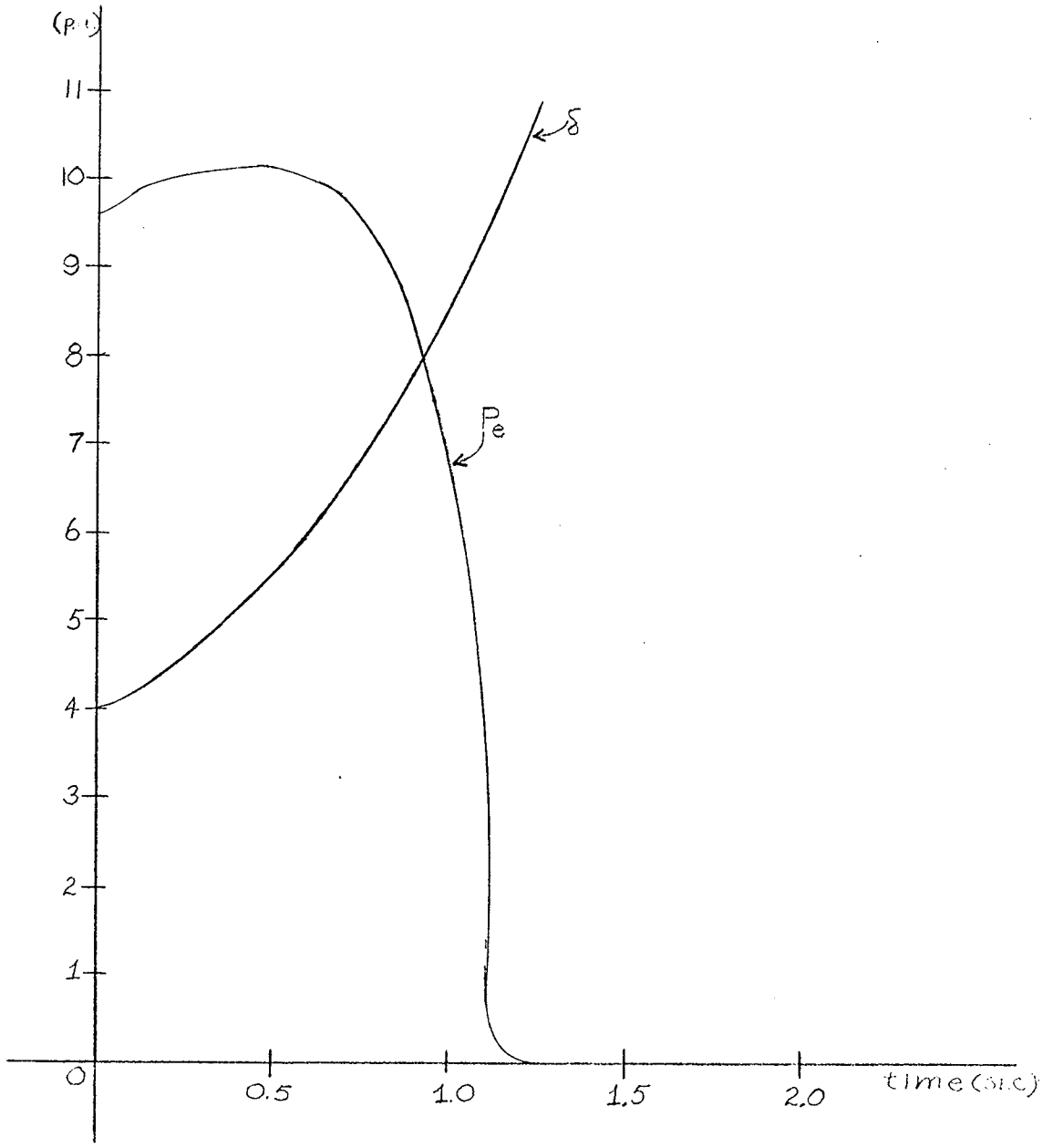

Fig. 5-5: Output trace for step input causing instability

STEP VOLTAGE INPUT STABILITY LIMIT

Operating Point	Lossy Digital Model	Lossless Digital Model	Analog Model
0.0 volts	11 volts	8.6 volts	8.6 volts
2.5 volts	P = 4.3 volts	2.7 volts	2.1 volts
4.0 volts	4.3 volts	0.5 volts	0.3 volts

TABLE III: List of Step Voltage Stability Limit for Turbine and Governor Model

small either positive or negative that the system seems to just settle there. As this slope becomes slightly negative it causes positive feedback effect which at first increases gradually, but as the slope then gets more negative farther to the right of $\delta = 90^{o}$, get the large exponential increase as evidenced on this graph. The same effect can be seen in a digital plot of a system going unstable.

5.4 Results of a Two-Area Simulation

Output results consisting of P_e vs time and δ vs time plots are presented in Figures 5-6, 5-7, 5-8 and 5-9. Results are shown both for inputs at P_{m1} and P_{m2}. The step voltage input stability limits for P_{m1} and P_{m2} inputs are given in Table IV.

Upon examining these plots it was found that the oscillatory response as a function of time is different depending on whether you apply it to P_{m1} of area A or P_{m2} of area B. This is due to the different values of M_1 and M_2 for A and B. If the input step is at P_{m1}, since area B has a smaller M it can react faster to any disturbance, so that a disturbance on area A will effect area B as well.

For disturbances at P_{m2} on area B, since area A is much more sluggish than area B, the response will behave just as if area B was tied to an infinite bus as in model A since area A seems to be inflexible compared to area B. This is illustrated in Figures 5-8 and 5-9. A close examination of these graphs shows that this is exactly what happens in this case.

From Table IV, see the relative comparison of the step voltage stability limit values for the analog and digital cases. No

Operating Point	INPUT TO AREA A		INPUT TO AREA B	
	Digital Model	Analog Model	Digital Model	Analog Model
0.0 volts	20.0 volts	20.0 volts	-12.0 volts	-12.0 volts
2.5 volts	5.8 volts	5.5 volts	-3.1 volts	-3.0 volts
4.0 volts	+0.8 volts	0.8 volts	-0.5 volts	0.5 volts

TABLE IV: List of Step Voltage Stability Limits for a Two-Area Model

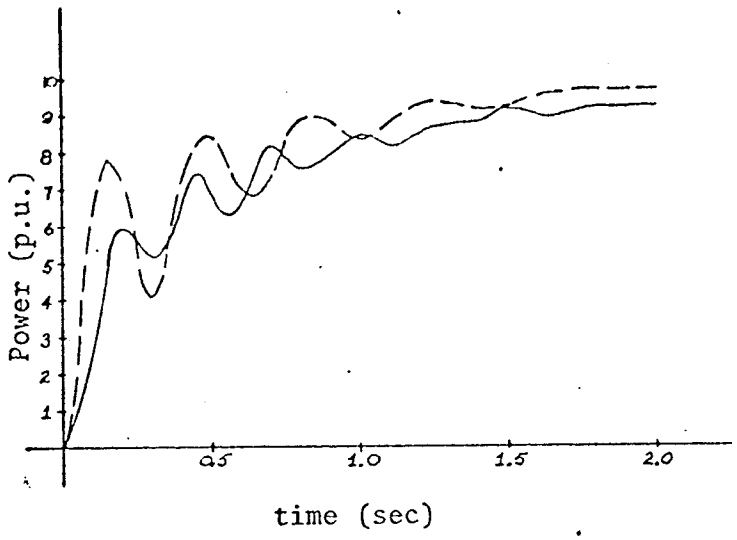

a) initial condition 0^{o}

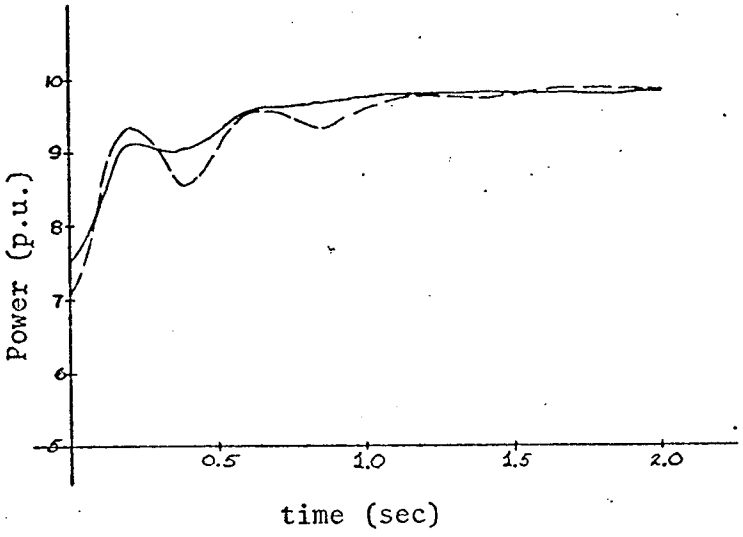

b) initial condition 45^{o}

Digital Lossy Case _ _ _ _

Analogue Case _____

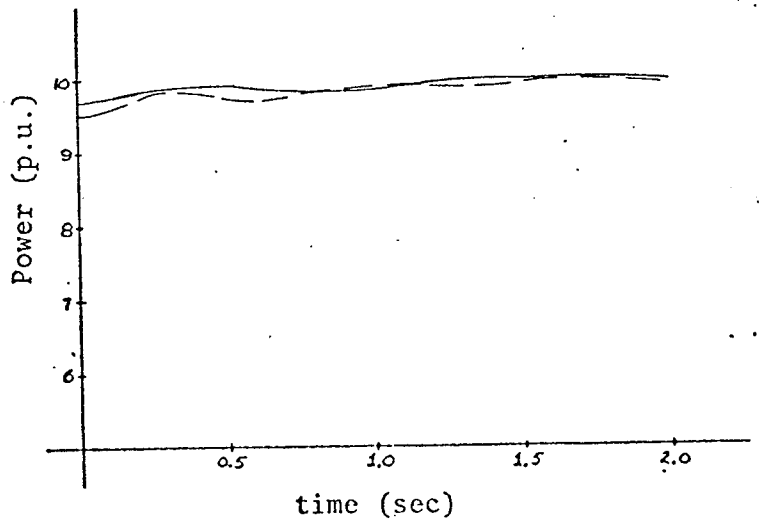

c) initial condition 72^{o}

Fig. 5-6: P_e vs time for Two Area Model with Step Input at P_{m1}.

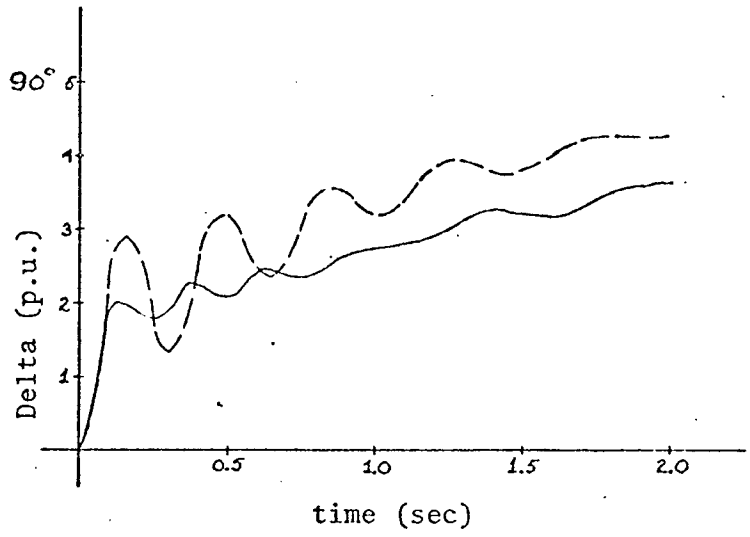

a) initial condition 0°

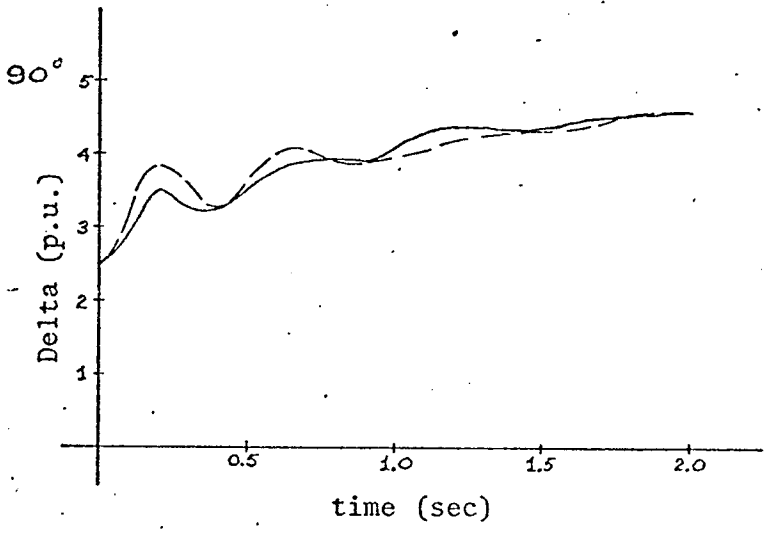

b) initial condition 45°

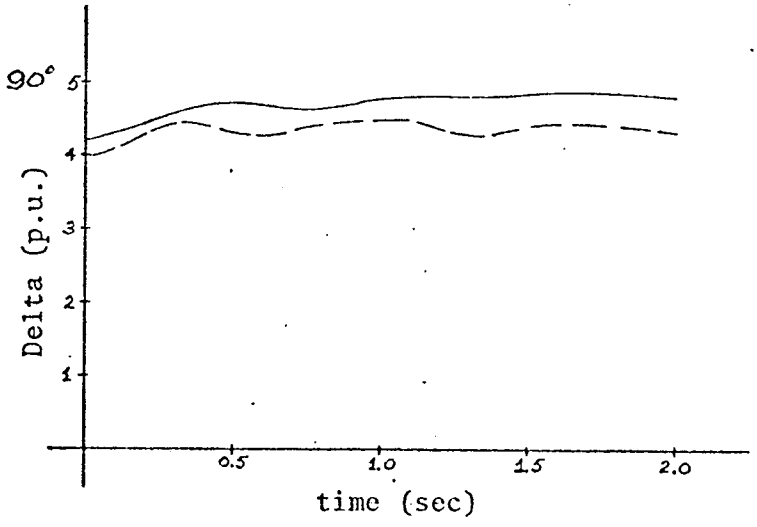

c) initial condition 72°

)igital Lossy Case

\nalogue Case

Fig. 5-7: δ vs time for Two-Area Model with Step Input at P_{m1}.

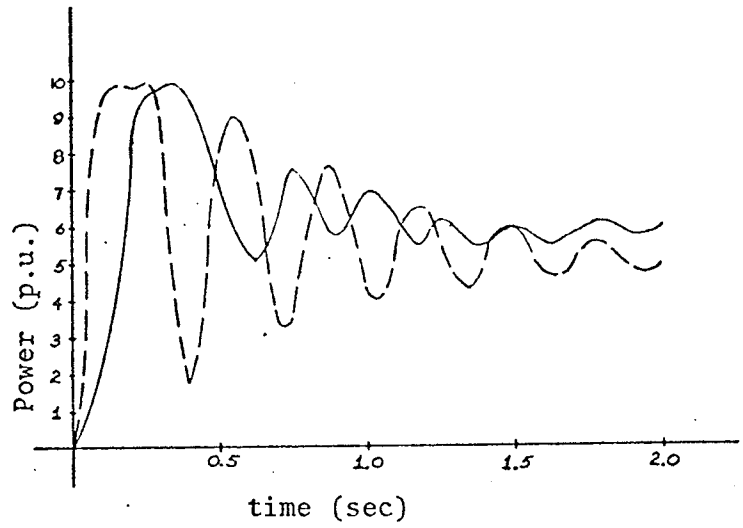

a) initial condition 0^{o}

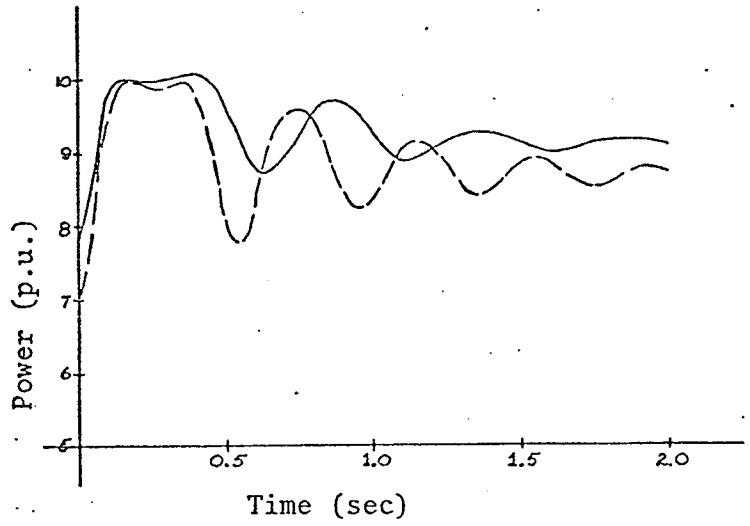

b) initial condition 45^{o}

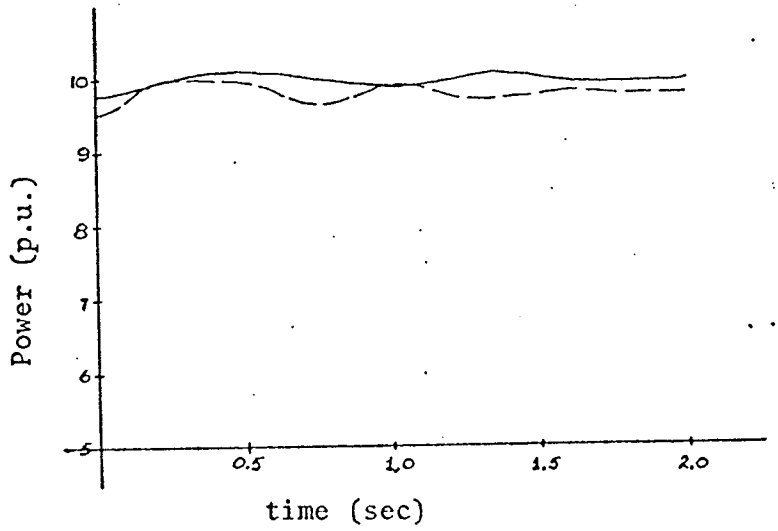

c) initial condition 72^{o}

Digital Lossy Case

Analogue Case

Fig. 5-8: P_e vs time for Two-Area Model with Step Input at P_{m2}.

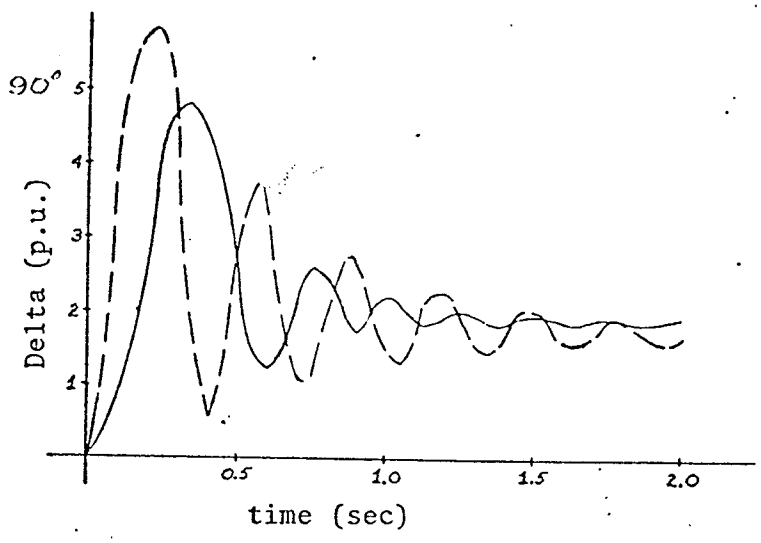

a) initial condition 0^{o}

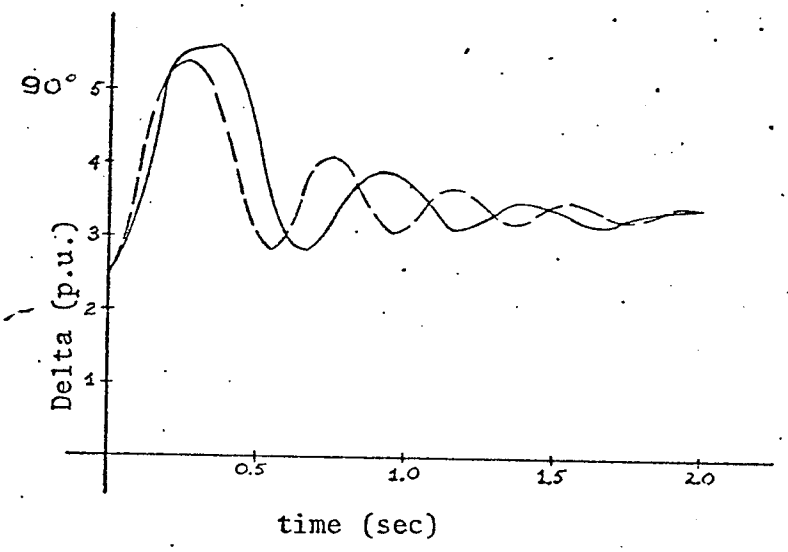

b) initial condition 45^{o}

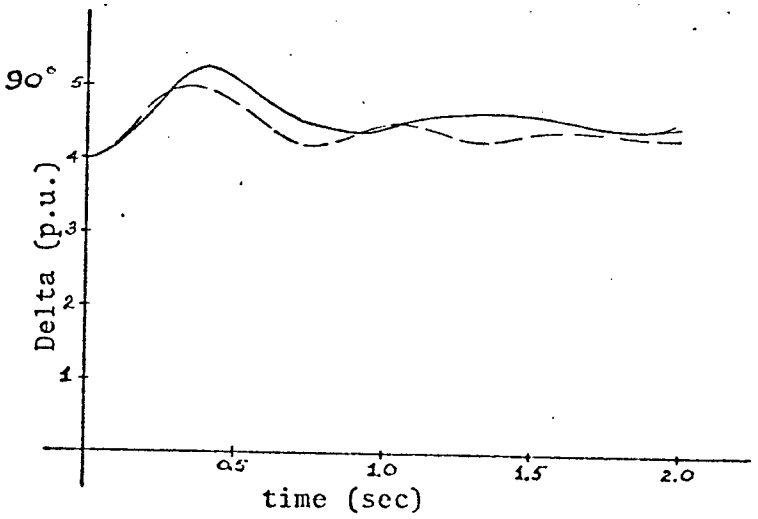

Digital Lossy Case — — —

Analogue Case ·····

c) initial condition 72^{o}

Fig. 5-9: δ vs time for Two-Area Model with Step Input at P_{m2}.

comparison was made with the lossy sine wave in this set of tests. In the case where step voltage is applied to area A, the values of stability limit are identical for both analog and digital simulation. This is due to the fact that the oscillations were quite small, therefore the power values of one model did not deviate drastically from that of the other, resulting in critical step voltages which are very nearly identical to one another.

A comparison of the step voltage stability limits between disturbances applied to area A and disturbances applied to area B indicate that the stability limits of a disturbance on area A were quite a bit higher than off those on area B. This can be explained by looking at the comparable oscillatory behavior of the two. For disturbances on area A, an exponentially increasing value with a damped sinusoid superimposed on it occurs.

For disturbances on area B on the other hand, the response has a high initial overshoot which causes the system to go unstable at much lower voltage values than in the other instances.

If it seems the analog oscillographs have faster settling times, it was only because the X-Y recorder vertical scale required for satisfactory operation did not show the small oscillations after the first few since they were too small to register well on the recordings.

It is interesting to note as a conclusion to this chapter that the analog system representation using the approximate sine wave model built yields quite good results when compared to those of the digital simulation.

This strengthens a person's confidence in this model thus allowing him to use it in more complex and detailed system studies.

CHAPTER 6: CONCLUSION

From the results of the system simulation, it can be concluded that this load-frequency model representation for the analog computer is quite accurate, if the digital simulation can be used as a valid comparison. Looking at percent error, in first-swing-peak, for different cases: Two-Bus System, Two-Bus with Governor System, and Two-Area System, the percent errors are as listed below

CASE	CURVE	ERROR
Two-Bus System	P vs t	5.3%
	δ vs t	10.0%
Two-Bus with Governor System	P vs t	8.7%
	δ vs t	14.0%
Two-Area System	P vs t	25.0%
	δ vs t	30.0%
	P vs t	5.0%
	δ vs t	20.0%

These errors, although they seem quite large, were for peak magnitude only and what this thesis was mostly concerned with was a Power Stability limit comparison which proved to be quite a bit more accurate.

There were differences in transient stability power limit but these were due to the errors in the nonlinear function representation. The errors were no larger than 5% for all cases except for the

45^{o} operating point in the Two-Bus Cases where they went as high as 20%. The reason for this discrepancy occurring was explained in Chapter V. If a more accurate model is desired it could be built using more line segments and hardware components of much higher tolerances. These refinements would cost additional money and it is debatable whether this increase in accuracy could reasonably be justified.

It is also quite possible that other techniques could be used to simulate this nonlinearity, but a search of pertinent analog computer books such as Blum (21), Rekoff (26) and Stephenson (35) do not indicate any other technique which would be conducive to modeling functions of this nature. It seems that in pretty well all applications of this kind where nonlinearities are involved, the diode function generator is the element used to generate the nonlinearity. Also since a technique almost identical to this one was suggested in a Russian publication by Sokolov, Gurevich and Khvoshchenskaya (16) it is a further indication that the method used is reasonable.

Once a model of the system has been developed the next course of action might be the testing of this model in a hybrid system. A more complex model incorporating many buses of a system (using a nonlinear model for each bus) could be developed on a large analog computer and this model could be intertied through A/D and D/A interfacing equipment with a minicomputer. This type of computer system could be used to study different problems such as the following; the effect of interconnection on the control system, the effect of power system "loops" on the load frequency control (the control of phase shifting transformer), the effect of system dynamics on the load frequency control (excitation-stabilization-system loops) and the effect of interaction with the HVDC control scheme.

BIBLIOGRAPHY

(1) R. Gorez, "Reglages Optimaux des Generateurs de Fonctions a Diodes", 4th International Analogue Computation Meetings, pp 241-244, 1964.

(2) C. E. Hart, "Improved Function Generation Subprograms for Use with CSMP or Other Digital Simulation Programs", Simulation Magazine, August 1971, pp 77-79.

(3) O. W. Hanson. C. J. Goodwin and P. L. Dandero, "Influence of Excitation and Speed Control Parameters in Stabilizing Intersystem Oscillations", IEEE Trans. Power Apparatus and Systems, Vol Pas-87 No 5, May 1968, pp 1306-1313.

(4) Nathan Cohn, "Methods of Controlling Generation on Interconnected Power Systems", AIEE Trans. Power Apparatus and Systems, Vol Pas-80, part III, June 1961, pp 270-282.

(5) Nathan Cohn, "Some Aspects of Tie-Line Bias Control on Interconnected Power Systems", AIEE Trans. Power Apparatus and Systems, Vol Pas-76, part III, pp 1415-1428, 1957.

(6) P. Thompson and R. Billington, "Generating Capacity Benefits Associated with Power Systems Interconnections", EIC Journal, October 1971.

(7) H. E. Lokay and R. L. Bolger, "Effect of Turbine-Generator Representation in System Stability Studies", IEEE Trans. Power Apparatus and Systems, Vol Pas-84, No 10, pp 933-942, Oct. 1965.

(8) H. E. Brown, R. B. Shipley, D. Coleman and R. W. Nied Jr., "A Study of Stability Equivalents", IEEE Trans. Power Apparatus and Systems, Vol Pas-88, No 3, March 1969, pp 200-207.

(9) K. Ganesan, J. J. Regehr and R. J. Fleming, "Optimization of Speed-Governor Parameters in the Presence of Pseudorandom Load Disturbances", IEEE Trans. Power Apparatus and Systems, Vol Pas-89, No 6, July/August 1970, pp 1242-1247.

(10) W. J. Smolinski, "Critical Damping Levels of a Hydraulic Turbine Generator" EIC Journal, Vol 12, Sept 1969.

(11) T. E. Harras and R. J. Fleming, "Optimal Adjustment of Hydraulic Turbine Governor by the Method of Krasovskii", EIC Journal, Vol 12, No C-4, May 1969.

(12) T. E. Harras, R. J. Fleming, "Single Machine Equivalents for Multimachine Hydro Plants", EIC Journal, Vol 11, No C-4, October 1968.

(13) M. H. Chaudhry and E. Ruus, "Analysis of Governing Stability of Hydroelectric Power Plants" EIC Journal, Vol 13, No C-5, June 1970.

(14) L. M. Hovey and L. A. Bateman, "Speed Regulation Tests on a Hydro Station Supplying an Isolated Load", AIEE Trans. Power Apparatus and Systems, Vol Pas-81, October 1962, pp 364-371.

(15) L. M. Hovey "Optimum Adjustment of Hydro Governors on Manitoba Hydro System", IEEE Trans. Power Apparatus and Systems, Vol Pas-81 October 1962, pp 364-371.

(16) N. I. Sokolov, Yu. E. Gurevich, Z. G. Khvoshchenskaya, "A New Method of Studying Large Complex Power Systems on Analogue Computers", Electric Technology USSR, Permagon Press Translations, Vol 2, 1961, pp 193-212.

(17) R. Tomovic and W. J. Karplus, High Speed Analog Computers, John Wiley and Sons Inc., New York, 1962.

(18) R. M. Howe, Design Fundamentals of Analog Computer Components, C. Van Nostrand Company Inc., New Jersey, 1961.

(19) L. Levine, Methods for Solving Engineering Problems Using Analog Computers, McGraw Book Company, 1964.

(20) C. L. Johnson, Analog Computer Techniques, McGraw-Hill Book Company Inc. 1956.

(21) J. J. Blum, Introduction to Analog Computation, Harcourt, Brace and World Inc., 1968.

(22) C. A. A. Wass, Introduction to Electronic Analogue Computers, Permagon Press Ltd., 1955.

(23) G. A. Korn and J. M. Korn, Electronic Analog Computers, McGraw-Hill Book Company Inc., 1956.

(24) J. E. Stice and B. S. Swanson, Electronic Analog Computer Primer, Blaisdell Publishing Company, 1965.

(25) A. S. Jackson, Analog Computation, McGraw-Hill Book Company Inc., 1960.

(26) M. G. Rekoff Jr., Analog Computer Programming, Charles E. Merrill Books Inc., 1967.

(27) Z. Nenadal and B. Mirtes, Analogue and Hybrid Computers, Iliffe Books Ltd., 1968.

(28) V. Borský and J. Malyás, Computation by Electronic Analogue Computers, Iliffe Books Ltd., 1968.

(29) J. N. Warfield, Introduction to Electronic Analog Computers, Prentice-Hall Inc., 1959.

(30) W. H. Carpenter, Solutions of Problems in Electrical Power Technology, Sir Isaac Pitman and Sons Ltd., 1968.

(31) D. I. Rummer, Introduction to Analog Computer Programming, Holt, Rinehart and Winston Inc., 1969.

(32) M. L. James, G. M. Smith and J. C. Wolford, Analog and Digital Computer Methods, International Textbook Company, 1964.

(33) W. D. Stevenson Jr., Elements of Power System Analysis, McGraw-Hill Book Company, 1962.

(34) O. I. Elgerd, Electric Energy Systems Theory: An Introduction, McGraw-Hill Book Company, 1971.

(35) R. E. Stephenson, Computer Simulation for Engineers.

APPENDIX A

Derivation of Power Loss Term

Consider two voltage sources as being tied together through a resistance and reactance as shown in Fig.

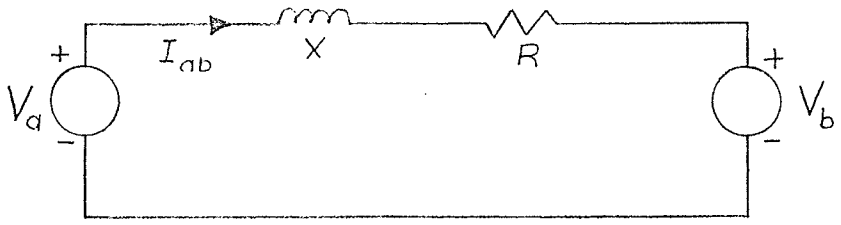

The current I_{AB} flowing in this circuit can then be represented by the expression

$$I_{ab} = \frac{V_a - V_b}{R + jX} \tag{1}$$

The equation for power loss can then be expressed as

$$P_L = |I_{ab}|^2 R$$

$$= \left|\frac{V_a - V_b}{R + jX}\right|^2 R = \left|\frac{|V_a| \cos\delta_{ab} + j|V_a| \sin\delta_{ab} - |V_b|}{R^2 + X^2}\right|^2$$

$$= \frac{(|V_a| \cos\delta_{ab} - |V_b|)^2 + (|V_a| \sin\delta)^2}{R^2 + X^2}$$

$$= \frac{R}{R^2 + X^2} \left| |V_a|^2 \cos^2\delta_{ab} - 2\,|V_a||V_b| \cos\delta_{ab} + \right.$$

$$\left. |V_b|^2 + |V_a|^2 \sin^2\delta \right| \tag{3}$$

$$= \frac{R}{R^2 + X^2} \left|V_a\right|^2 + \left|V_b\right|^2 - 2\left|V_a\right|\left|V_b\right| \cos \delta \qquad (4)$$

This expression for P_L is also equivalent to $(P_{ab} + P_{ba})$

Also P_e (transmitted power) $= P_{ab} - P_\ell$

$$P_e = \frac{1}{R^2 + X^2} [-R \left|V_b\right|^2 + R \left|V_a\right|\left|V_b\right| \cos \delta_{ab} +$$

$$X \left|V_a\right|\left|V_b\right| \sin \delta_{ab}] \qquad (5)$$

This expression is equivalent to the equation for power flowing into bus B referenced from bus A (i.e. $-P_{ab}$).

This substantiates the claim that the expression for P_{ab} is an expression for the power transfer capability from buses A to B including line losses. If the losses are removed from the expression to determine the actual power received at bus B equation 5 results. Assuming R to be zero (no losses) then the expression for P_e becomes the original lossless formula

$$P_e = \frac{V_a \ V_b}{X} \cos \delta \qquad (6)$$

```
      DIMENSION  DIV(13),X(120),VERT(120),V(120)
      DOUBLE PRECISION DIV,X,VERT,V,DX,H,VT,S,T,Y,B,A,DSIN
      READ (5,1000) VMAX,NDIV,NSECT
 1000 FORMAT (F6.3,I4,I1)
      READ (5,2000) (DIV(I),I=1,NSECT)
 2000 FORMAT (F6.3)
      DX = VMAX/NDIV
      V(1) = 0.0
      NDIG= NDIV+1
      DO 100 I = 2,NDIG
  100 V(I)=V(I-1)+DX
      DO 200 I=1,NDIG
      X(I)=3.14159*(V(I)/180.0)
  200 VERT(I)=10.0*DSIN(X(I))
      LL=1
      K=0
      J=0
  300 J=J+1
      K=K+1
      Z=NSECT-1
      IF (J.GT.Z) GO TO 700
      LOW=LL
      H=0.0
      S=0.0
      T=0.0
      VT=0.0
      DO 400 I=LOW,NDIG
      LL=I
      G=J+1
      IF (V(I).GT.DIV(G)) GO TO 500
      H=H+VERT(I)
      VT=VT+V(I)
      S=S+V(I)**2.0
      T=T+V(I)*VERT(I)
  400 CONTINUE
  500 Y=10*(DIV(K+1)-DIV(K))
      B=(T-((H*VT)/Y))/(S-((VT**2.0)/Y))
      A=(H-(B*VT))/Y
      WRITE (6,3000) H,VT,S,T,B,A,Y
 3000 FORMAT (4E12.6,2E16.6,E6.3)
      IF (LOW.LT.NDIG) GO TO 300
  700 CONTINUE
      WRITE (6,12)(DIV(I),I=1,NSECT)
   12 FORMAT (F6.3)
      STOP
      END
```

APPENDIX B - LEAST-SQUARED ERROR ANALYSIS PROGRAM

```
            ****CONTINUOUS SYSTEM MODELING PROGRAM****

      ***PROBLEM INPUT STATEMENTS***

FUNCTION SINE=-10.0,-5.91,-9.5,-6.89,-9.0,-8.03,-8.5,-9.04,-8.0,-9.91...
         ,-7.5,-10.61,-7.0,-11.12,-6.5,-11.42,-6.0,-11.52,-5.5,-11.41...
         ,-5.0,-11.09,-4.5,-10.57,-4.0,-9.86,-3.5,-8.99,-3.0,-7.97,-2...
         .5,-6.82,-2.0,-5.58,-1.5,-4.27,-1.0,-2.94,-0.5,-1.60,0.0,0.0...
        ,0.5,1.60,1.0,2.94,1.5,4.27,2.0,5.58,2.5,6.82,3.0,7.97,3.5,8....
         99,4.0,9.87,4.5,10.57,5.0,11.09,5.5,11.41,6.0,11.52,6.5,11....
         42,7.0,11.12,7.5,10.61,8.0,9.91,8.5,9.05,9.0,8.03,9.5,6.89,1...
         0.0,5.91
CONST    M=0.33,D=-0.33,A=100,PIC=6.82
TIMER    DELT=0.05,FINTIM=5.0,PRDEL=0.05,OUTDEL=0.05
PARAM    PIN=(3.4,3.5,3.6,3.7)
         PM=PIN+PR+PIC
         RA=M*PM
         RB=D*OMEGA
         OMEGA=INTGRL(0.0,RC)
         RC=RA+RB
         LINE=A*OMEGA
         DELTA=INTGRL(2.5,LINE)
         PE=AFGEN(SINE,DELTA)
         PR=PE*(-1.0)
PRTPLT   PE
LABEL    POWER VERSUS TIME
PRTPLT   DELTA
LABEL    DELTA VERSUS TIME
END
STOP
```

APPENDIX C - CSMP PROGRAM FOR SWING EQUATION MODEL

```
****CONTINUOUS SYSTEM MODELING PROGRAM****

***PROBLEM INPUT STATEMENTS***

FUNCTION SINE=-10.0,0.0,-9.5,-1.56,-9.0,-3.09,-8.5,-4.53,-8.0,-5.
         -7.5,-7.07,-7.0,-8.09,-6.5,-8.91,-6.0,-9.51,-5.5,-9.88,-5
         -10.0,-4.5,-9.87,-4.0,-9.51,-3.5,-8.91,-3.0,-8.09,-2.5,-7
         -2.0,-5.88,-1.5,-4.54,-1.0,-3.09,-0.5,-1.56,0.0,0.0,0.5,1
         1.0,3.09,1.5,4.53,2.0,5.88,2.5,7.07,3.0,8.09,3.5,8.91,4.0
         9.51,4.5,9.87,5.0,10.0,5.5,9.87,6.0,9.51,6.5,8.91,7.0,8.0
         7.5,7.07,8.0,5.88,8.5,4.54,9.0,3.09,9.5,1.56,10.0,0.0
CONST    M=1.0,D=-1.0,A=33.,PIC=7.07,TTA=10.0,TTB=10.0,TGA=10.0,TG
TIMER    DELT=0.05,FINTIM=3.50,PRDEL=0.05,OUTDEL=0.05
         PC=0.0
PARAM    PI=(2.0,2.2,2.4,2.5,2.7)
         X=PC+PA
         XA=X*(TGA)
         XC=XA+XB
         Y=INTGRL(0.0,XC)
         XB=Y*(-TGB)
         YA=Y*(TTA)
         YC=YA+YB
         PIN=INTGRL(0.0,YC)
         YB=PIN*(-TTB)
         PA=PINE*(-10.0)
PARAM    HL=0.01
         PIL=HL*PIN
         PM=PIL+PR+PIC+PI
         RA=M*PM
         RB=D*OMEGA
         OMEGA=INTGRL(0.0,RC)
         RC=RA+RB
         PINE=A*OMEGA
         G=1.0
         LINE=PINE*G
         DELTA=INTGRL(2.5,LINE)
         PE=AFGEN(SINE,DELTA)
         PR=PE*(-1.0)
PRTPLT   PE
LABEL    POWER VERSUS TIME
PRTPLT   DELTA
LABEL    DELTA VERSUS TIME
END
PARAM    HL=0.1
END
STOP
```

APPENDIX D - CSMP PROGRAM FOR TURBINE AND GOVERNOR INCLUDED MODEL

```
****CONTINUOUS SYSTEM MODELING PROGRAM****

***PROBLEM INPUT STATEMENTS***

FUNCTION SINE=-10.0,0.0,-9.5,-1.56,-9.0,-3.09,-8.5,-4.53,-8.0,-5.88,...
         -7.5,-7.07,-7.0,-8.09,-6.5,-8.91,-6.0,-9.51,-5.5,-9.88,-5.0,...
         -10.0,-4.5,-9.87,-4.0,-9.51,-3.5,-8.91,-3.0,-8.09,-2.5,-7.1,...
         -2.0,-5.88,-1.5,-4.54,-1.0,-3.09,-0.5,-1.56,0.0,0.0,0.5,1.6,...
         1.0,3.09,1.5,4.53,2.0,5.88,2.5,7.07,3.0,8.09,3.5,8.91,4.0,...
         9.51,4.5,9.87,5.0,10.0,5.5,9.87,6.0,9.51,6.5,8.91,7.0,8.09,...
         7.5,7.07,8.0,5.88,8.5,4.54,9.0,3.09,9.5,1.56,10.0,0.0
CONST    M=1.0,D=-1.0,A=33.,PIC=0.00
CONST    SF=4.0,SG=+4.0,AA=33.
TIMER    DELT=0.05,FINTIM=5.00,PRDEL=0.05,OUTDEL=0.05
PARAM    PIL=0.00
         PM=PIL+PR+PIC+PI
         PI=0.0
         RA=M*PM
         RB=D*OMEGA
         RC=RA+RB
         OMEGA=INTGRL(0.0,RC)
         PINE=A*OMEGA
         GX=1.0
         LINE=PINE*GX
PARAM    PC2=0.0
         FB=0.00
         G=FB+PC2+PR2-PIC
         GA=G*SF
         GC=GA+GB
         GD=INTGRL(0.0,GC)
         GB=GD*(-SG)
         GG=GD*AA
         GH=GG*(-1.0)
         Z=LINE+GH
         ZZ=1.0*Z
         DELTA=INTGRL(0.0,ZZ)
         PE=AFGEN(SINE,DELTA)
         PR=PE*(-1.0)
         PR2=PE*(+1.0)
PRTPLT   PE
LABEL    POWER VERSUS TIME
PRTPLT   DELTA
LABEL    DELTA VERSUS TIME
END
PARAM    PIL=(20.6,20.7,20.8,20.9)
END
STOP
```

APPENDIX E - CSMP PROGRAM FOR TWO-AREA MODEL